Bull. Mater. Sci., Vol. 1, Numbers 3 and 4, December 1979, pp. 129–170. © Printed in India.

Soft modes and structural phase transitions*

G VENKATARAMAN
Reactor Research Centre, Kalpakkam 603 102

MS received 19 June 1978

Abstract. This paper presents a survey of soft modes and their relationship to structural phase transitions. After introducing the concept of a soft mode, the origin of softening is considered from a lattice-dynamical point. The Landau theory approach to structural transitions is then discussed, followed by a generalisation of the soft-mode concept through the use of the dynamic order-parameter susceptibility. The relationship of soft modes to broken symmetry is also examined. Experimental results for several classes of crystals are next presented, bringing out various features such as the co-operative Jahn–Tellev effect. The survey concludes with a discussion of the central peak, touching upon both the experimental results and the theoretical speculations.

1. Introduction

I am grateful for this opportunity to discuss soft modes and structural phase transitions. Although I have never worked in this area, I used to keep abreast of this subject in view of my interest in lattice dynamics, but lately I began to lose touch. The present assignment has enabled me to pick up the threads again and become aware of the excitement sweeping the field.

Historically speaking, Raman and Nedungadi (1940) seem to have been the first to observe a soft mode in a structural phase transition. This was not generally well-known in the past, and I became aware of it when Prof. Chandrasekhar mentioned it at the Academy meeting in the year following Prof. Raman's death. It is gratifying that this fact has now got into a book (Blinc and Zeks 1974), ensuring better recognition to Raman's pioneering contribution. The next important event in the history of soft modes is undoubtedly the prediction made independently by Cochran (1959) and Anderson (1960) that phase transitions in certain ferroelectrics might result from lattice dynamical instability. Great excitement was aroused when soon after this, Cowley (1962) discovered in his neutron scattering experiments on $SrTiO_3$ that one of the $q = 0$ optic modes showed a softening behaviour as the temperature was decreased. Unfortunately, there was no concomitant (ferroelectric) phase transition but a soft mode and a related phase transition were discovered in $SrTiO_3$ a little later. The subject of soft modes soon became wide open, a variety of experimental techniques like NMR, ERR, light scattering,

* Survey presented at the discussion meeting on phase transitions arranged by the Indian Academy of Sciences at Bangalore in June 1978.

neutron scattering, etc. being applied to a study of the problem. In 1971, fresh excitement was aroused through the discovery of a central peak accompanying the soft mode, leading to renewed vigour on both the experimental and theoretical fronts. In view of all this, it is appropriate that we spend some time at this meeting to catch up with what has transpired in this field.

2. General aspects of soft modes

Let us begin with the question, "what is a soft mode?". Operationally, one may define the soft mode as a collective excitation whose frequency decreases anomalously as the transition point is reached. On account of its historical association, the term soft mode always brings to mind a lattice dynamical mode but, as we shall see later, one could have other types of soft modes as well. Further, softening could occur not only as one approaches the transition temperature from above but also from below. In what follows, we shall by and large restrict attention to lattice dynamical soft modes. Such modes trigger a lattice instability, leading to a structural phase transition either of a second or first order.

Table 1 offers a brief classification of the structural changes that could ensue. In some cases, such changes are accompanied by the onset of either ferroelectricity or antiferroelectricity. I shall not be overly concerned with the ferroelectric aspects of these phase transitions since Prof. Srinivasan will be covering them in his presentation.

Figure 1 shows a schematic of the different kinds of soft modes that have been observed so far. Of interest is the result for Nb_3Sn where a sizable chunk of a whole branch goes soft. Experience todate regarding the spectral character of the soft mode is summarised in figure 2 from which one finds that the mode can be either underdamped or overdamped (depending on the anharmonicity prevailing). Figure 3 gives a schematic view of the temperature dependence of the soft mode frequency. It is to be noted that whereas in a second-order transition, the soft

Table 1. Classification of structural phase transitions with typical examples.

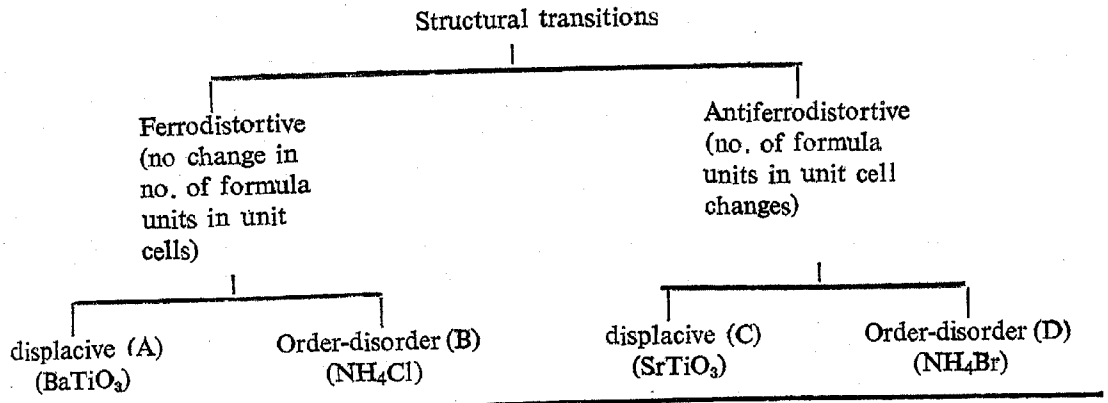

Note : 1. A reference to Blinc and Zeks (1974) will show that in category A, only ferroelectrics seem to occur. In category C, both ferroelectrics and antiferroelectrics are possible.

2. Birgeneau *et al* (1974) mention that there is a third group of transitions in which there is a strong coupling between order-disorder and displacive types of variables. Examples cited are KDP and $PrAlO_3$.

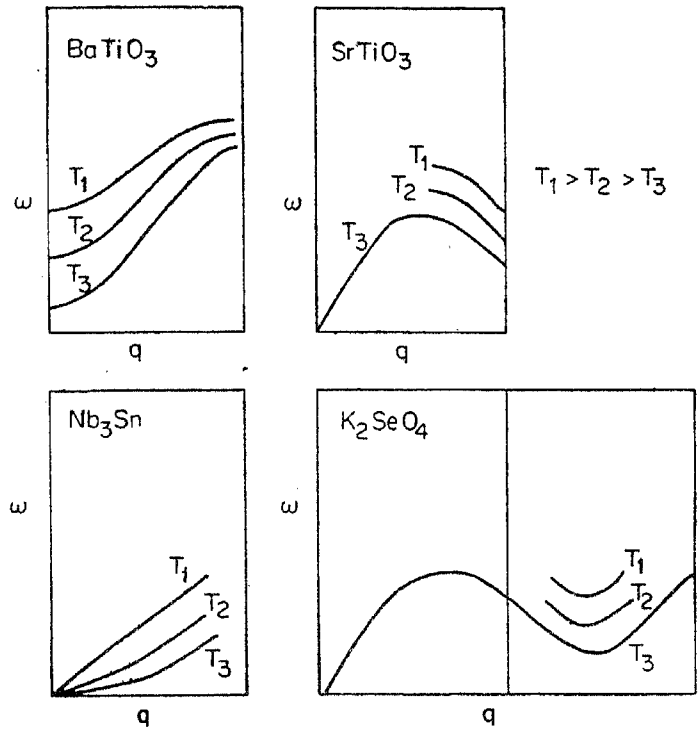

Figure 1. Schematic drawings of the various kinds of soft modes observed so far. Notice the softening can occur anywhere in the Brillouin zone. Examples of materials exhibiting such behaviour are also given.

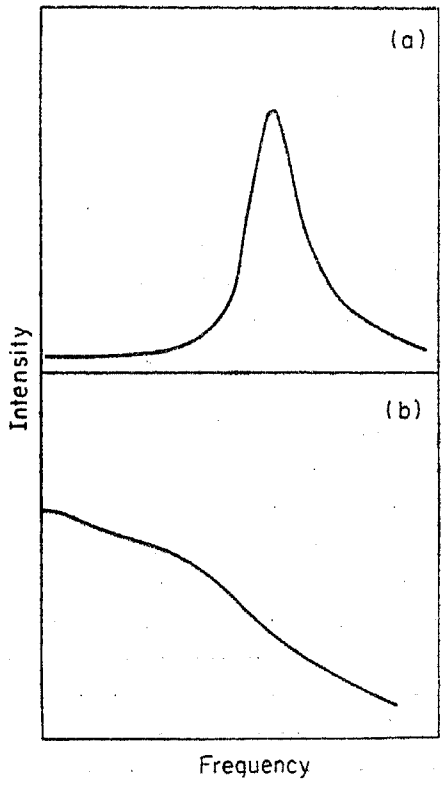

Figure 2. Typical lineshapes of soft modes. (*a*) corresponds to underdamped, and (*b*) to overdamped modes.

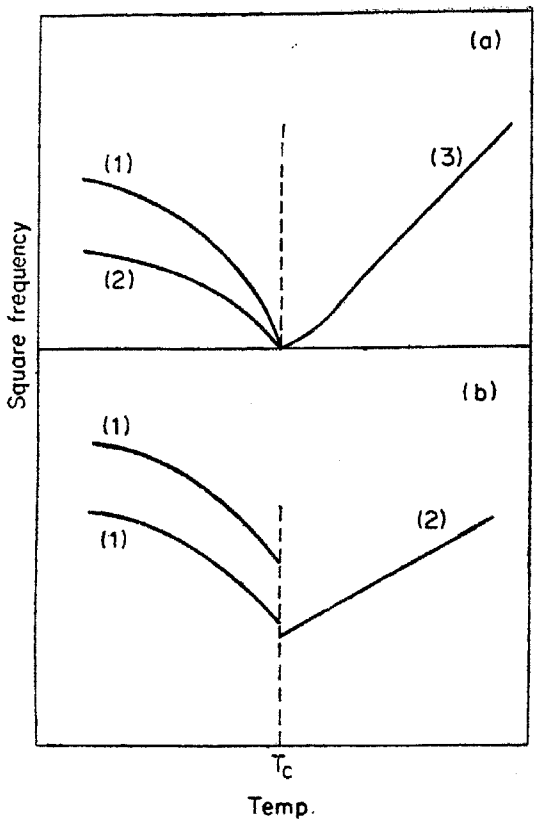

Figure 3. Variation of soft mode frequency with temperature for (*a*) second-order and (*b*) first-order transitions. The numbers in parenthesis denote degeneracy.

mode frequency actually vanishes at the transition point, in a first-order transition, the change of phase occurs before the mode frequency is *able* to go to zero.

Attention is drawn to the fact that soft modes exist also below T_c. This is not unexpected because if the structural transition is due to the condensation of a soft mode that exists above T_c, then correspondingly there must be agencies below T_c which seek to restore the symmetry of the high-temperature phase as temperature is increased from below T_c. Thus it is that as many soft modes appear below T_c as exist above T_c.

We next consider the order parameter associated with structural phase transitions, and their relation to the soft modes. The concept of the order parameter will be formally introduced later but for the moment let us discuss some qualitative aspects without being too fussy about the definition.

The order parameter, as all of us know, is a measure of the order resulting from the phase transition. We shall denote it by the symbol ψ. In all structural phase transitions, the average value of ψ denoted by $\langle \psi \rangle$ is non-vanishing below T_c and vanishes above T_c. The change is continuous across the transition temperature for a second-order transition, and is discontinuous for a first-order transition (figure 4). It is important to realise that ψ itself is not a static quantity even though $\langle \psi \rangle$ is. Thus ψ can fluctuate, and in fact these fluctuations are derived by a suitable superposition of the atomic displacements associated with the soft mode vibrations. The fluctuations are so organised that $\langle \psi \rangle$ vanishes identically in the high-tempera-

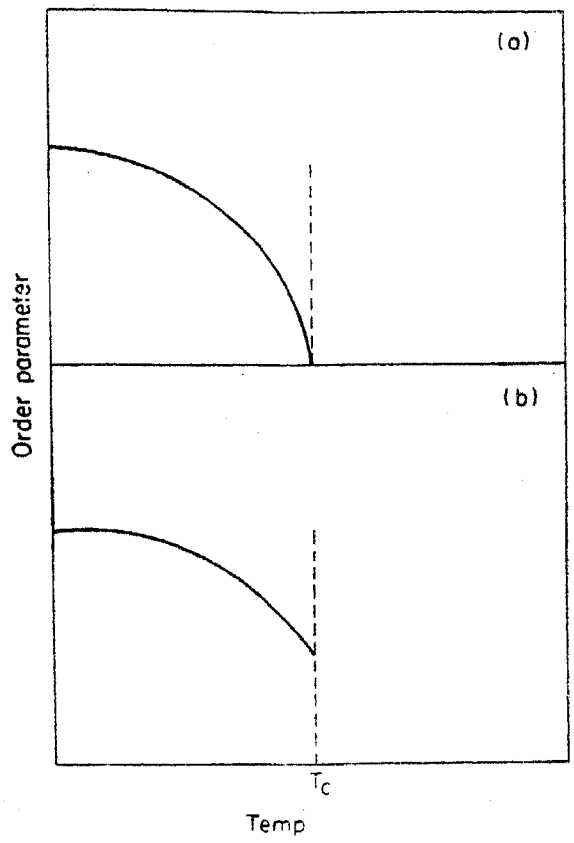

Figure 4. Variation of the order parameter with temperature for (*a*) second-order and (*b*) first-order transitions.

ture phase but becomes non-vanishing in the low-temperature phase. The fluctuations become important near T_c and diminish as one moves away from T_c on either side. Correspondingly, the soft modes also become *stiffer*.

3. Softening from a lattice dynamics point

Having noted the existence of soft modes, the next question obviously is, "why do modes become soft ?" This can be tackled in a variety of ways and we shall start with the lattice dynamists' approach.

Many years ago, Born (see Born and Huang 1954) established that a crystal lattice will become unstable if one of its normal-mode frequencies becomes purely imaginary. Let us pursue this line of argument. Now the lattice dynamical Hamiltonian is usually written in the form (Venkataraman *et al* 1975)

$$H = \frac{1}{2} \sum_{\mathbf{q}j} \left\{ P\begin{pmatrix}\mathbf{q}\\ j\end{pmatrix} P\begin{pmatrix}-\mathbf{q}\\ j\end{pmatrix} + \omega_0^2\begin{pmatrix}\mathbf{q}\\ j\end{pmatrix} Q\begin{pmatrix}\mathbf{q}\\ j\end{pmatrix} Q\begin{pmatrix}-\mathbf{q}\\ j\end{pmatrix} \right\}, \tag{1}$$

where the Q's denote the normal coordinates and the P's the conjugate momenta. The Hamiltonian of equation (1) is purely harmonic and since anharmonic effects play a crucial role in the softening process, the above Hamiltonian obviously needs

to be enlarged. Assuming for simplicity only fourth-order anharmonic effects (a common practice), the above Hamiltonian may be expanded to an effective Hamiltonian of the form

$$H_{\text{eff}} = \frac{1}{2}\sum_{\mathbf{q}j}\left\{P\begin{pmatrix}\mathbf{q}\\ j\end{pmatrix}P\begin{pmatrix}-\mathbf{q}\\ j\end{pmatrix}+\omega_0^2\begin{pmatrix}\mathbf{q}\\ j\end{pmatrix}Q\begin{pmatrix}\mathbf{q}\\ j\end{pmatrix}Q\begin{pmatrix}-\mathbf{q}\\ j\end{pmatrix}\right\}$$
$$+\sum_{\mathbf{q},\kappa}\sum_{jklm}V^4_{jklm}(\mathbf{q},\kappa)\left\langle Q\begin{pmatrix}\mathbf{q}\\ j\end{pmatrix}Q\begin{pmatrix}-\mathbf{q}\\ k\end{pmatrix}\right\rangle Q\begin{pmatrix}\kappa\\ l\end{pmatrix}Q\begin{pmatrix}-\kappa\\ m\end{pmatrix}. \tag{2}$$

In the above, the usual fourth-order term has been replaced by one of the form $\langle QQ'\rangle Q''Q'''$ so as to define an effective quadratic potential for the phonons. It is possible in principle to diagonalise (2) to the form

$$H_{\text{eff}} = \frac{1}{2}\sum_{\mathbf{q}j}\left\{\bar{P}\begin{pmatrix}\mathbf{q}\\ j\end{pmatrix}\bar{P}\begin{pmatrix}-\mathbf{q}\\ j\end{pmatrix}+\bar{\omega}^2\begin{pmatrix}\mathbf{q}\\ j\end{pmatrix}\bar{Q}\begin{pmatrix}\mathbf{q}\\ j\end{pmatrix}\bar{Q}\begin{pmatrix}-\mathbf{q}\\ j\end{pmatrix}\right\}, \tag{3}$$

where $\bar{\omega}$ denotes the renormalised mode frequency, and is related to the bare frequency ω_0 by

$$\bar{\omega}^2\begin{pmatrix}\mathbf{q}\\ j\end{pmatrix}=\omega_0^2\begin{pmatrix}\mathbf{q}\\ j\end{pmatrix}+2\sum_{\kappa}\sum_{lm}V^4_{jjlm}(\mathbf{q},\kappa)\left\langle Q\begin{pmatrix}\kappa\\ l\end{pmatrix}Q\begin{pmatrix}-\kappa\\ m\end{pmatrix}\right\rangle. \tag{4}$$

Let $(\mathbf{q}, j)$ denote the soft mode, and we further suppose that the forces in the crystal are such as to make $\bar{\omega}_0^2\begin{pmatrix}\mathbf{q}\\ j\end{pmatrix}$ negative. However, from experiments we know that $\bar{\omega}^2$ for the soft mode must be positive. This is obviously possible only if the anharmonic effects represented by the second term on the r.h.s. of (4) overwhelm the negative contribution from ω_0^2. It now becomes conceivable that as temperature is lowered, the anharmonic contribution may not be able to counter the effects of ω_0^2 sufficiently. In turn this would lead to $\bar{\omega}^2$ becoming negative, producing in its wake a crystal instability, as required by Born's theorem. Nature of course averts this disaster by bestowing a different structure, better conducive to lattice stability.

An estimate for the transition temperature may be obtained from equation (4) (Blinc and Zeks 1974). On evaluating the $\langle\cdots\rangle$ term on the r.h.s., one obtains

$$\bar{\omega}^2\begin{pmatrix}\mathbf{q}\\ j\end{pmatrix}=\omega_0^2\begin{pmatrix}\mathbf{q}\\ j\end{pmatrix}+2\sum_{l\kappa}V^4_{jjll}(\mathbf{q},\kappa)\frac{1}{2\bar{\omega}\begin{pmatrix}\kappa\\ l\end{pmatrix}}$$
$$\times\coth\left[\frac{1}{2}\beta\bar{\omega}\begin{pmatrix}\kappa\\ l\end{pmatrix}\right]\left(\beta=\frac{1}{k_\beta T},\ \hbar=1\right). \tag{5}$$

Since the renormalised frequency occurs on both sides, one has obviously a self-consistency problem. An approximate solution could however be obtained by replacing $\bar{\omega}$ by ω_0 on the r.h.s. leading to the result

$$\bar{\omega}^2\begin{pmatrix}\mathbf{q}\\ j\end{pmatrix}\approx\omega_0^2\begin{pmatrix}\mathbf{q}\\ j\end{pmatrix}+2\sum_{l\kappa}{}'V^4_{jjll}(\mathbf{q},\kappa)\left[2\omega_0\begin{pmatrix}\kappa\\ l\end{pmatrix}\right]^{-1}\coth\left[\frac{1}{2}\beta\omega_0\begin{pmatrix}\kappa\\ l\end{pmatrix}\right]. \tag{6}$$

Notice the prime on the summation on r.h.s. This implies the exclusion of soft modes which is necessary as their bare frequencies are purely imaginary. Assuming now that $\omega_0 \ll k_B T$, we can recast the above as

$$\bar{\omega}^2 \text{ (soft mode)} \sim a\,(T - T_c), \tag{7}$$

where $$a = k_B \sum_{l\kappa}{}' V^4_{jlll} \Big/ \omega_0 \left(\frac{\kappa}{l}\right), \tag{8}$$

and $$T_c = -\,[\omega_0^2 \text{ (soft mode)}/a], \tag{9}$$

denotes the transition temperature. It is worth emphasising that by their very nature, the soft modes are expected to make substantial contributions to anharmonic effects which, however, have been carefully excluded in (6) ! The above exercise is therefore not good for quantitative purposes although it serves well as a plausibility argument. Methods are of course available to accommodate the anharmonic effects contributed by the soft modes but we shall not discuss them here.

4. Landau's theory

There is another way of looking at structural phase transitions, and that is via Landau's theory. Landau and Lifshitz (1959) discuss this at some length in their classic book on statistical physics—and many of you may already be familiar with it. So I shall content myself with presenting a bare outline, adequate for the present purpose.

In a second-order phase transition, the change of state is continuous (*i.e.* order parameter changes continuously). Taking note of this, Landau assumed that the Gibb's free energy $g\,(T, P, \psi)$ in the neighbourhood of the transition point should be expandable as a series in powers of a certain quantity ψ, the order parameter. To arrive at the nature of this expansion, Landau and Lifshitz consider the density $\rho\ (x,\ y,\ z)$ which describes the probability distribution of atom positions in the crystal. ρ then must evidently reflect the symmetry group of the crystal which means that for $T > T_c$, ρ must be consistent with the symmetry group G_0 of the high-temperature phase. Likewise, for $T < T_c$, ρ must be consistent with the group G_0 of the low-temperature phase. This enables one to write

$$\rho = \rho_0 + \delta\rho, \tag{10}$$

where ρ_0 corresponds to the symmetry of G_0 and ρ to the symmetry of G. It is clear that $\delta\rho$ has the same symmetry as ρ. Using group-theoretic arguments, Landau and Lifshitz then show that $\delta\rho$ may be written

$$\delta\rho = \sum_i C_i \phi_i^{\lambda}\,(\Gamma_\lambda), \tag{11}$$

where ϕ_i^{λ} are basis functions which transform according to the irreducible representation Γ_λ of G_0. The index i runs over the set of such functions.

Now the Gibb's free energy g will not only be a function of temperature and pressure but also of ρ and hence of the coefficients C_i. Introducing the notation

$$\psi^2 = \sum_i C_i^2,\ C_i = \gamma_i \psi \text{ (so that } \sum_i \gamma_i^2 = 1), \tag{12}$$

the free energy expansion upto fourth order is written in the form*

$$g = g_0 + A\psi^2 + \psi^4 \sum_a V_a f_a^4(\gamma_i). \tag{13}$$

Here ψ is the order parameter informally introduced earlier and now defined by (12). The quantity f_α^4 is an invariant of fourth order constructed from γ_i. Such invariants occur when g is expanded in terms of the C_i's because g itself is invariant under the symmetry group of the crystal. The sum over a in (13) contains as many terms as there are individual invariants of corresponding order.

The stable state of the crystal is found by minimising g with respect to ψ and γ_i. The stability conditions are:

$$\partial g/\partial\psi = 0, \quad \partial^2 g/\partial\psi^2 > 0. \tag{14}$$

Nothing has been said so far about the sign of the coefficients of the ψ^2 and ψ^4 terms. Landau and Lifshitz show that the coefficient of ψ^4 must always be positive; also it is not strongly temperature-dependent. A on the other hand varies rapidly with temperature and can have any sign. The state $\langle\psi\rangle = 0$ (no order) is stable for $A > 0$ whereas when $A < 0$, $\langle\psi\rangle$ is non-vanishing**. Transition from high symmetry G_0 to low symmetry G accompanied by the appearance of an order parameter $\langle\psi\rangle$ thus occurs when A changes sign.

Figure 5 shows a sketch of g in various situations. The appearance of the double well explains why $\langle\psi\rangle$ becomes non-vanishing below T_c.

Several footnotes must now be added to the above discussion. Firstly, in the context of soft modes, the basis functions entering the expansion (11) will be eigenvectors of the soft mode of the high symmetry phase. If the wave-vector of the soft mode is $\mathbf{q}$, then i runs over all the partners corresponding to the irreducible representation $\Gamma_\lambda(\mathbf{q})$ of the wave-vector group $G_0(\mathbf{q})$ and over similar sets corresponding to all other wave-vectors belonging to the star of $\mathbf{q}$.

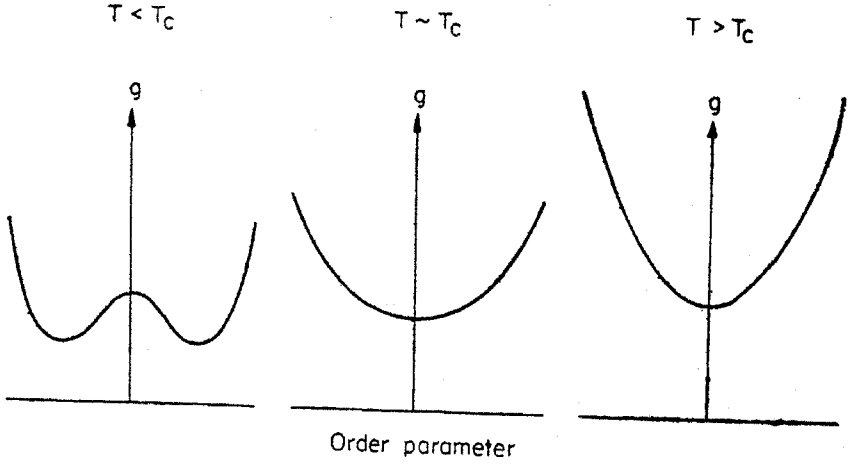

Figure 5. Schematic drawing of the behaviour of the free energy g as a function of the order parameter in various temperature regimes.

* The odd terms are ruled out by suitable arguments !

** Note in the Landau theory there is no difference between ψ and $\langle\psi\rangle$ since the order parameter does not fluctuate.

Next we note that (13) is often applied to a first-order phase transition, but for this a sixth order term must be added with positive coefficient, and the coefficient of the fourth-order term must be negative.

If the order parameter (which is derived from the soft-mode eigenvectors), transforms like a polar vector, then a non-vanishing value for ψ could lead to a non-vanishing value for the polarisation P and hence to ferroelectricity. In this situation, one could effectively replace ψ by P in the free energy expansion (apart from scaling factors of course).

Sometimes more than one mode may go soft in which case, the expansion (11) must extend to all such modes. We shall see one example of this later.

We observed above that in ferroelectrics, ψ and P are synonymous. This, however, is not always true. Ferroelectrics are known where the order parameter is not the spontaneous polarisation. Similarly, there could be other properties like macroscopic strain which manifest in the low symmetry phase but which do not constitute the order parameter. Such quantities (which may be regarded as subsidiary order parameters) appear on account of coupling with ψ. To deal with such cases, the free energy expansion must include these subsidiary parameters also, and correspondingly, the stability conditions (14) must be augmented. Later I shall cite an example.

One other point I would like to add concerning (13) is that if all the coefficients are known (corresponding to a given thermodynamic state), then the soft mode frequencies may be determined from the secular equation

$$\| D_{ij} - \omega_\lambda^2 \delta_{ij} \| = 0, \tag{15}$$

where $$D_{ij} = \partial^2 g / \partial \psi_i \partial \psi_j, \quad \psi_i = \psi \gamma_i. \tag{16}$$

The derivative in (16) is evaluated around the minimum of g.

Reviewing the theoretical framework as a whole, we see that there are two basic approaches. The first starts from a model Hamiltonian and focusses attention on the lattice dynamical aspects. Landau's theory on the other hand revolves round an order parameter and emphasises the phase transition aspects. There have been some attempts (e.g. Pytte 1972) to synthesise the two. Experimentalists, on the other hand, exploit Landau's theory extensively because they can in favourable cases determine the soft-mode eigenvectors directly from experiments.

5. Generalisation of the soft-mode concepts

We have so far associated softening behaviour exclusively with lattice vibrational modes. Schneider *et al* (1972) generalised this concept to several other situations by combining the static aspects of phase transitions (as revealed through divergences in appropriate susceptibilities) with the dynamic response of the system (as manifested via the dynamic susceptibility). To understand their work, a few definitions are necessary.

First we consider the static susceptibility $\chi_{\psi\psi}$ with respect to the order parameter which is defined operationally by considering a small external field $V_{ext}(\mathbf{r}) = V_0 \exp(i\mathbf{q} \cdot \mathbf{r})$ which couples to the local order parameter $\psi(\mathbf{r})$. Following Kubo (1966), the response $\delta\psi(\mathbf{r})$ may be expressed as

$$\delta\psi(\mathbf{r}) = \int \chi_{\psi\psi}(\mathbf{r}, \mathbf{r}') V_{ext}(\mathbf{r}') \, d\mathbf{r}', \tag{17}$$

where $\chi_{\psi\psi}(\mathbf{r}, \mathbf{r}')$ is the *static*, order-parameter response function, and may be expressed in terms of order-parameter correlations $\langle \psi(\mathbf{r}) \psi(\mathbf{r}') \rangle$. For a system that is translationally invariant,

$$\chi_{\psi\psi}(\mathbf{r}, \mathbf{r}') \to \chi_{\psi\psi}(\mathbf{r} - \mathbf{r}').$$

Near a phase transition

$$\chi_{\psi\psi}(\mathbf{q}) = \int \exp(i\mathbf{q}\cdot\mathbf{r}) \chi_{\psi\psi}(\mathbf{r})\, d\mathbf{r}, \tag{18}$$

diverges for some $\mathbf{q}$. A divergence at $q = 0$ is associated with the existence of a long wave-length order parameter while a similar divergence at some non-zero wave-vector $\mathbf{q}_c$ (= zone boundary, for example), implies correspondingly an order parameter of finite wavelength.

Turning next to the dynamical behaviour of the system, one could consider a *weak* time-dependent external field $V_{\text{ext}}(\mathbf{r}, t) = \lim_{\eta \to 0} V \exp(\eta t) \exp i(\mathbf{q}.r - \omega t)$ switched on adiabatically from $t = -\infty$. The response will be linear in the perturbation and given by

$$\langle \delta\psi(\mathbf{r}, t) \rangle = \lim_{\eta \to 0} \int d\mathbf{r}' \int_{-\infty}^{t} dt' \chi''_{\psi\psi}(\mathbf{r} - \mathbf{r}',\ t - t')\, V_{\text{ext}}(r',\ t'). \tag{19}$$

The complex susceptibility $\chi_{\psi\psi}(\mathbf{q}, z)$ is related to the above response by

$$\chi_{\psi\psi}(\mathbf{q}, z) = P \int_{-\infty}^{\infty} \frac{d\omega}{\pi} \frac{\chi''_{\psi\psi}(\mathbf{q}, \omega)}{\omega - z}. \tag{20}$$

Schneider *et al* (1972) point out that if the total number of degrees of freedom is large compared to the degrees of freedom associated with ψ, then the latter may be regarded as an ergodic variable. Using this assumption they show

$$\chi_{\psi\psi}(\mathbf{q}) = \lim_{\epsilon \to 0} \chi_{\psi\psi}(\mathbf{q}, z)\,|_{z = i\epsilon}, \tag{21}$$

where $\chi(q)$ is derived from the *static* response function defined earlier, and $\chi(q, z)$ is the *dynamic* response introduced above. In other words, if the order parameter is an ergodic variable, then the isothermal susceptibility that one usually considers in the context of phase transitions can be expressed as above as an appropriate limit of the dynamic susceptibility. The question now is whether the singular behaviour of $\chi(q)$ near a phase transition can be related to features in the dynamics through a general consideration of the properties of the dynamic susceptibility. The answer is obtained if one considers the result

$$\chi_{\psi\psi}(q) = \chi_{\psi\psi}(q, z = 0) = \mathbf{P} \int_{-\infty}^{\infty} \frac{d\omega}{\pi} \frac{\chi''(q, \omega)}{\omega},$$

and the expression

$$\int_{-\infty}^{\infty} \frac{d\omega}{\pi} \omega\chi''(q, \omega),$$

for the first moment of $\chi''_{\psi\psi}$. Schneider *et al* (1972) remark that "in any equilibrium phase, the first moment of $\chi''_{\psi\psi}$ exists and is finite". The only way in which

the area under (χ''/ω) can diverge while that under $(\omega^2 \chi''/\omega)$ remains finite is if the main contribution to the former comes from small ω, i.e. if (χ''/ω) is peaked for small ω. In other words, for the desired behaviour, at least one of the poles of $\chi(q, z)$ has to move towards the origin (cf. figure 6) implying that a collective mode becomes soft. Note, however, that as per present discussion softening requires that not only the real part but also the imaginary part of the collective mode must vanish at the transition point. Among other things, this opens up the possibility of viewing diffusive modes (which will have zero centre frequency but a finite width due to relaxation) as soft modes in appropriate situations. Schneider *et al* (1972) make the further observation that in any given transition between two phases I and II, the same physical quantity might be responsible for the instability occurring when one goes from I to II as from II to I. However, the manifestation of the soft modes might be different in the two phases, e.g. diffusive in one and propagative in the other. These concepts are applied by Schneider *et al* (1972) to a number of well-known phase transitions (like spin flop and superfluid transitions), to identify the corresponding soft modes.*

6. Soft modes and broken symmetry

In my presentation, I have been asked to make some comments on the broken symmetry aspects of soft modes.

The idea of symmetry-breaking was first introduced in the context of particle physics by Goldstone (1961) who conjectured that if a continuous symmetry group leaves the Lagrangian invariant but not the vacuum, then there must exist zero

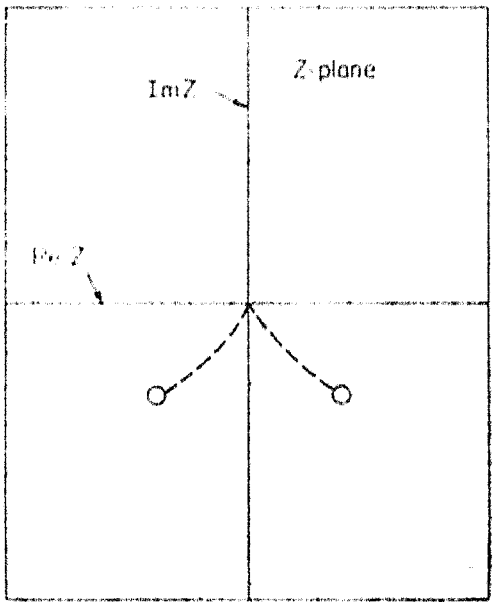

Figure 6. March of the poles of $\chi(q, z)$ towards the origin as the temperature is varied. Such a behaviour for the poles implies the existence of a soft mode subject to the condition ψ is ergodic.

* To complete the picture it must be pointed out that Thomas (1974) has expressed doubts about ψ being ergodic in the low-symmetry phase.

mass spinless particles. The proof was subsequently given by Goldstone *et al* (1962) and extended to non-relativistic case by Lange (1966) and Katz and Frishman (1966). A good discussion of the subject in relation to condensed matter has been given by Forster (1975; see also Anderson 1963).

Let Q be a Hermitian operator which is the integral of a local operator $q(\mathbf{r}, t)$, i.e.

$$Q = \int d\mathbf{r}\, q(\mathbf{r}, t).$$

We assume Q commutes with the Hamiltonian which means that Q is a constant of motion i.e. a generator of *continuous* transformations $U(\phi) = \exp(i\phi Q/\hbar)$ under which the Hamiltonian is invariant. Next let us further assume that there exist two other Hermitian operators $A(\mathbf{r})$ and $B(\mathbf{r})$ such that

$$\frac{1}{i\hbar}[Q, A(\mathbf{r})] = B(\mathbf{r}). \tag{22}$$

If
$$\begin{aligned} B_0 &\equiv \langle \int B(\mathbf{r})\, d\mathbf{r} \rangle, \\ &= \mathrm{Tr}\, \rho_0 \int B(\mathbf{r})\, d\mathbf{r}, \\ &\neq 0 \qquad (\rho_0\text{-density matrix}), \end{aligned}$$

then it implies $[\rho_0, Q] \neq 0$. In other words, even though the Hamiltonian is invariant under the symmetry transformation Q, a particular realisation of the state of the system as exemplified by ρ_0 is *not* invariant under Q. In such a situation, the continuous symmetry Q is said to be broken, and B is referred to as the symmetry-breaking operator. A on the other hand, is referred to as the symmetry-restoring operator, and B_0 is termed the order parameter. The dynamics of A is of particular significance, and the essence of the Goldstone theorem as applied to condensed matter physics is that there exist collective excitations associated with A whose frequency $\omega \to 0$ as $q \to 0$: The excitations corresponding to the $q \to 0$ limit are usually referred to as Goldstone modes. Their zero frequency has a direct analogy with the zero mass of the Goldstone boson of field theory. One assumption which has tacitly been made in all this is that the effective forces acting in the medium are of short range.

The standard example cited to illustrate broken symmetry concepts is the (isotropic) ferromagnet. Here the Hamiltonian is invariant under rotations but the physical realisation of the ferromagnet (in which the spins are pointing say in the Z direction), is not; evidently one has a case of symmetry breaking. Since the symmetry that is broken is continuous, and since the forces are of short range, Goldstone modes may be expected. With reference to the formal discussion given a little earlier, the following identifications can be made in the case of the ferromagnet :

$$Q = \mathbf{S}_Y^{\mathrm{tot}}, \quad B(r) = M_Z(r), \quad A(r) = M_X(r) \tag{23}$$

where $\mathbf{S}^{\mathrm{tot}}$ denotes the total spin and $\mathbf{M}$ the magnetisation. The dynamics of A then leads to the following dispersion law (Forster 1975)

$$\omega = Dq^2, \tag{24}$$

which has the correct limiting behaviour expected of Goldstone modes. The branch as a whole is sometimes referred to as the Goldstone branch. The dispersion

relation in (24) is of course already familiar to us as that for spin waves. What the present discussion shows is that the long wavelength spin wave modes can also be interpreted as Goldstone modes since the transverse spin fluctuation has the effect of symmetry restoration (equations (22 and 23)).

With regard to the direction of alignment of spins, there is nothing special about the one assumed by us. Other alignments are also possible as sketched in figure 7, and the long wavelength spin wave is a mode that essentially takes the system from one configuration to another, i.e., rotates the spin. This process costs zero energy implying that the different configurations are energetically equivalent.

The above discussion has glossed over one point, namely, that the dispersion relation for spin waves is not quite what is given in (24) but has the form (Kittel 1963)

$$\omega = Dq^2 + CH_A$$

where H_A is anisotropy field and C is a suitable constant. The field H_A has the effect of locking the spins in a particular direction. The principal consequence of the anisotropy field is that a gap appears in the dispersion relations as sketched in figure 8. What is even more interesting is that as $T \to T_c$, the gap diminishes, strongly reminiscent of the soft mode behaviour.

The origin of the gap as due to anisotropic effects is of course the standard explanation. However, there are deeper implications (Anderson 1963). It is well-known (Opechowski and Guccione 1965) that the preferred state (i.e. one with specific spin alignment) is not invariant under time reversal, (which is a discrete symmetry). Anderson has pointed out that it is the breaking of the discrete symmetry which results in a favoured energy configuration separated from its neighbours by a finite gap. At this point, I shall quote Anderson's words: "It is important to notice that in general a *continuous* broken symmetry—translation, gauge, rotation—leads to $\omega \to 0$, and usually zero-point amplitude $\to \infty$ as $q \to 0$, whereas a discrete broken symmetry—such as time reversal in the case of magnets, or interchange of sublattices for order-disorder—need not have any special consequences for the collective modes of the condensed system, unless it happens that there is at least

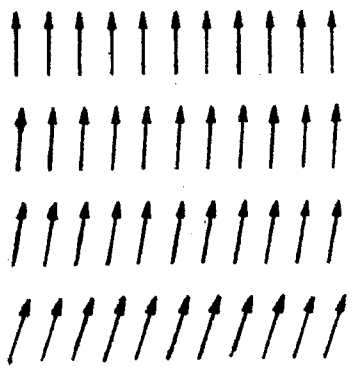

Figure 7. Several possible arrangements for spin alignment in a ferromagnet. These arrangements are all energetically equivalent (in the absence of external field and anisotropy field), and the $q = 0$ spinwave essentially takes the spin system slowly through a tour of these configurations.

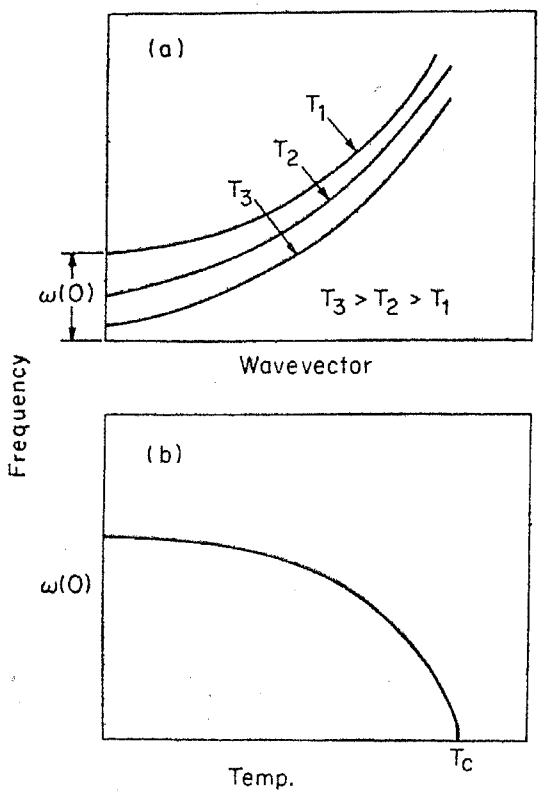

Figure 8. (*a*) Schematic of the spin wave dispersion relations in a ferromagnet at various temperatures. Observe the gap at $q = 0$. This arises due to the breaking of a discrete symmetry. In (*b*) is sketched the variation of the gap with temperature.

an approximate continuous symmetry-breaking, as occurs for the magnetic—and it happens also for the ferroelectric—cases". The rider above is important. Breaking of discrete symmetry (a common occurrence in structural phase transitions) *must* be accompanied by the breaking of continuous symmetry also. Only then can one talk of Goldstone modes which become finite frequency modes (on account of the breaking of some discrete symmetry). Blinc and Zeks (1974) also touch upon some of these concepts in their book.

Before leaving the subject, I would like to make one comment and that is that broken symmetry concepts are basically applied in the context of continuous symmetry-breaking. Anderson's remarks concerning what happens due to the additional presence of discrete symmetry-breaking is apparently a conjecture. I do not believe a formal discussion exists of such a joint symmetry-breaking. So the use of broken symmetry concepts *vis-a-vis* soft modes must, I think, be accepted with some caution.

7. Some experimental results

It is time we started looking at some experimental results to get a feel for the actual connection between soft modes and structural phase transitions. We shall begin with $SrTiO_3$ which has become almost a paradigm for displacive phase transitions.

7.1. $SrTiO_3$

$SrTiO_3$ has the perovskite structure (figure 9) and as mentioned in my introductory remarks, a soft mode at $q = 0$ was discovered by Cowley nearly sixteen years ago. However, this soft mode produced merely an enhancement of the dielectric constant and no phase transition. A second order cubic to tetragonal transition at $\sim$ 108 K was discovered in the substance, and guided by EPR experiments. Unoki and Sakudo (1967) suggested that it was presumably driven by an instability in some optic branch at large wave-ve tor. Based on Raman scattering experiments, Fleury *et al* (1968) subsequently made this suggestion into a concrete model and proposed that the softening occurred at the point R in the Brillouin zone (see figure 10). Figure 11 which shows the neutron scattering results of Shirane and Yamada (1969) confirmed this expectation.

Now the soft mode in the high-temperature phase is triply degenerate and transforms according to the representation R_{25} of the wave-vector group corresponding to R. From our earlier discussion we know that there must correspondingly be three soft modes in the low temperature phase. Indeed there are, and, on account of the effective doubling of the unit cell, these modes appear at $q = 0$. Figure 12 shows the temperature dependence of these modes. A pleasing feature is the good agreement between data obtained with quite different techniques. Figure 13 shows the temperature variation of the frequency of the A_{1g} mode and the order parameter (deduced from EPR experiments to be discussed later). These results may be compared with the qualitative curves sketched earlier.

Besides $SrTiO_3$, a number of other crystals having the pervoskite structure exhibit structural phase transitions. It is obviously not possible to give an exhaustive

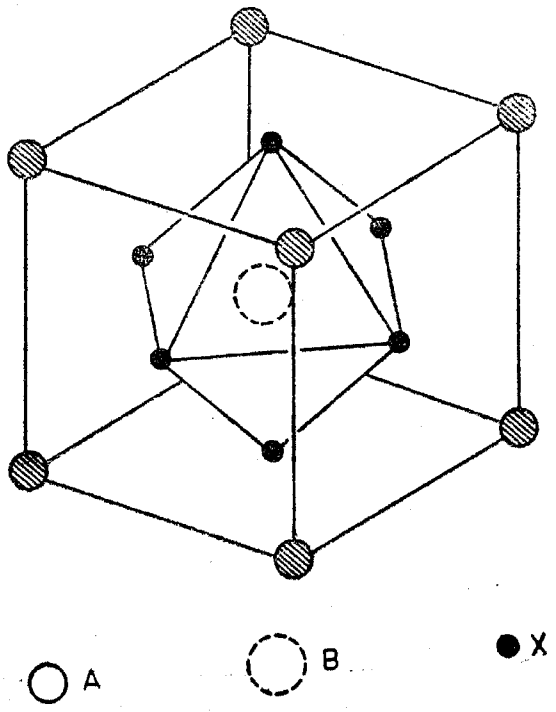

Figure 9. Sketch of the perovskite structure ABX_3 showing the octahedra of the X atoms.

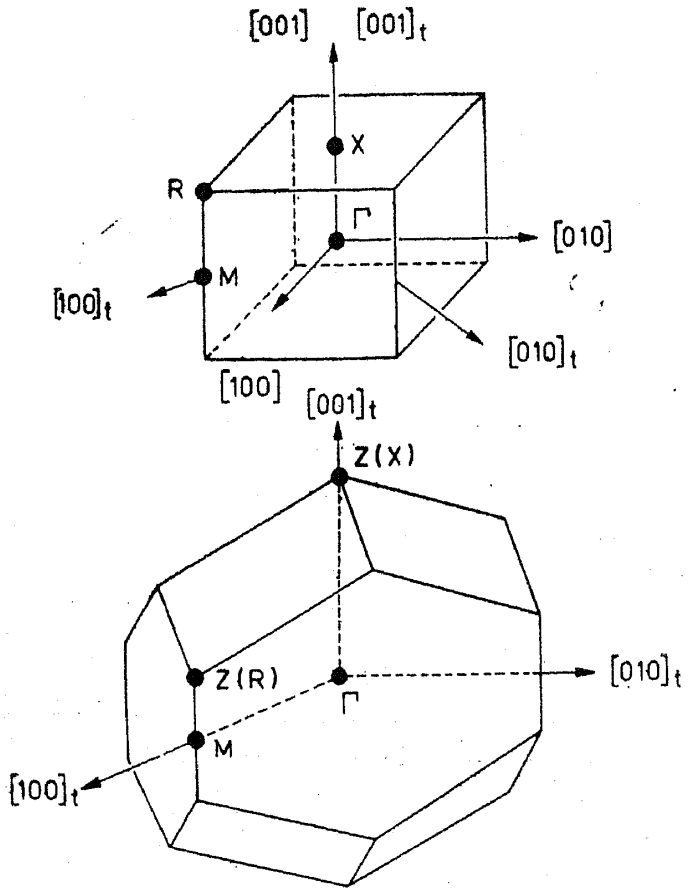

Figure 10. Brillouin zones of the cubic and tetragonal lattices. Note the axes for the two systems are rotated with respect to each other. In the tetragonal phase, the points X and R of the cubic Brillouin zone become equivalent.

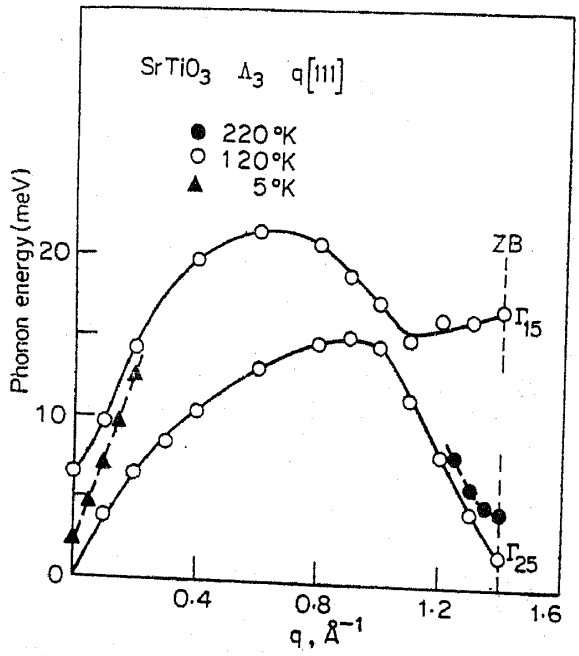

Figure 11. Soft modes in $SrTiO_3$ above T_c. (After Shirane and Yamada 1969).

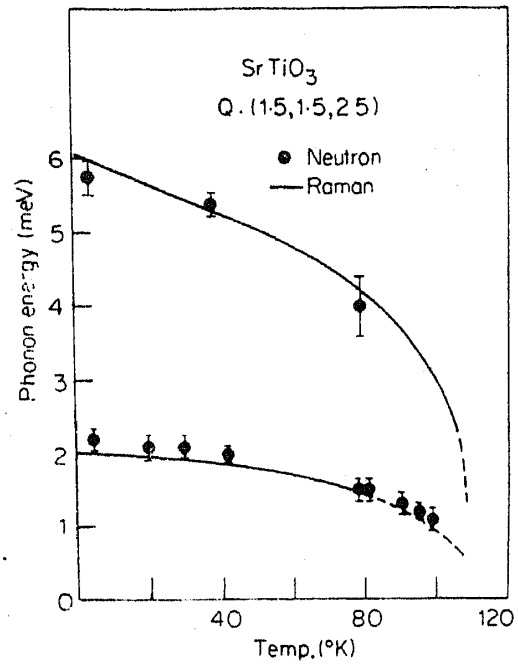

Figure 12. Soft modes in $SrTiO_3$ below T_c. (After Shirane and Yamada 1969).

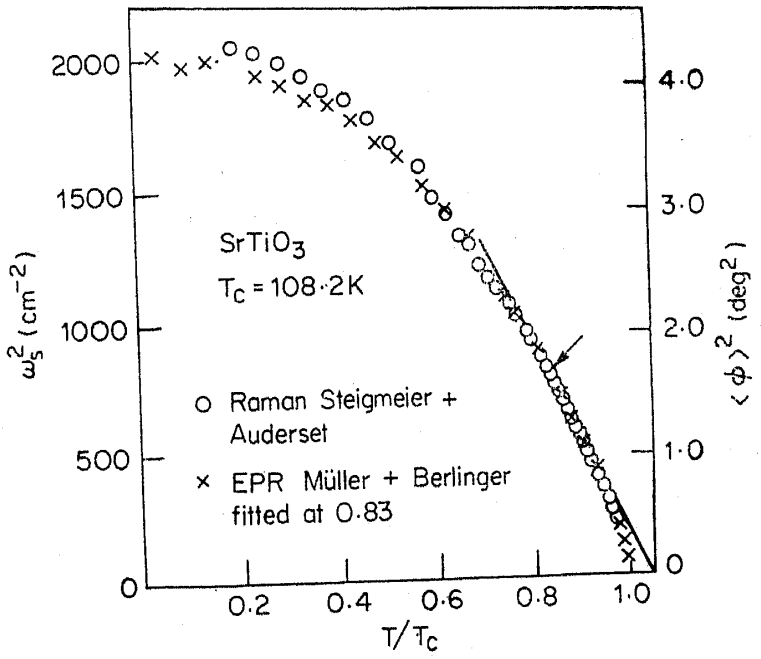

Figure 13. Temperature dependences of the square of the A_{1g} soft mode in $SrTiO_3$ (as determined from Raman scattering) and the square of the order parameter (as determined from EPR). (After Steigmeier *et al* 1974).

discussion of all these here, and I shall choose a few select examples to illustrate specific points.

7·2. *$LaAlO_3$*

$LaAlO_3$ also belongs to the perovskite group, and like strontium titanate, exhibits a second-order structural phase transition at ~ 800 K. As in $SrTiO_3$, the transi-

tion is driven by the condensation of phonons at the point R (Axe *et al* 1969) but an important difference is that the low-temperature phase has the rhombohedral structure rather than tetragonal. An analysis due to Thomas and Muller (1968) affords an explanation for this difference. To understand their work, a reference is first necessary to figure 14 which shows the structure of $SrTiO_3$ in the low temperature phase. The feature of interest is the rotation of the oxygen tetrahedra. The static rotation in the low-temperature phase is a direct consequence of the fact that the soft mode in the high-temperature phase, i.e. R_{25} involves rotational motions of the tetrahedra.

Thomas and Muller (1968) consider a free energy expansion of the form

$$g = g_0 + \tfrac{1}{2} A(\psi_x^2 + \psi_y^2 + \psi_z^2) + \tfrac{1}{4} B(\psi_x^4 + \psi_y^4 + \psi_z^4) + \\ + \tfrac{1}{2} C(\psi_x^2\psi_y^2 + \psi_y^2\psi_z^2 + \psi_z^2\psi_x^2). \qquad (25)$$

Here ψ_α $(\alpha = x, y, z)$ denotes the rotation of the tetrahedra about one of the cubic axes. The coefficient A is temperature dependent but B and C are not. By examining the stability for a range of parameter values, Thomas and Muller conclude that, depending on the values for B and C, both tetragonal and rhombohedral structures are feasible as sketched in figure 15. $SrTiO_3$ and $LaAlO_3$ provide actual demonstration of these two possibilities (see also figure 16).

7.3. *$CsPbCl_3$*

$CsPbCl_3$ offers an even more interesting case study. Here there are three phase transitions, particulars of which are given in table 2. Neutron scattering experiments by Fujii *et al* (1974) have revealed that the transition at 47° C is triggered by the non-degenerate phonon M_3 going soft (figure 17). The second transition at 42° C is associated with the condensation of the phonon Z_5^x at the point Z in the zone boundary along the [001] direction of the tetragonal lattice. Z_5^x is a member of the degenerate pair (Z_5^x, Z_5^y) derived from the R_{25} mode of the cubic phase

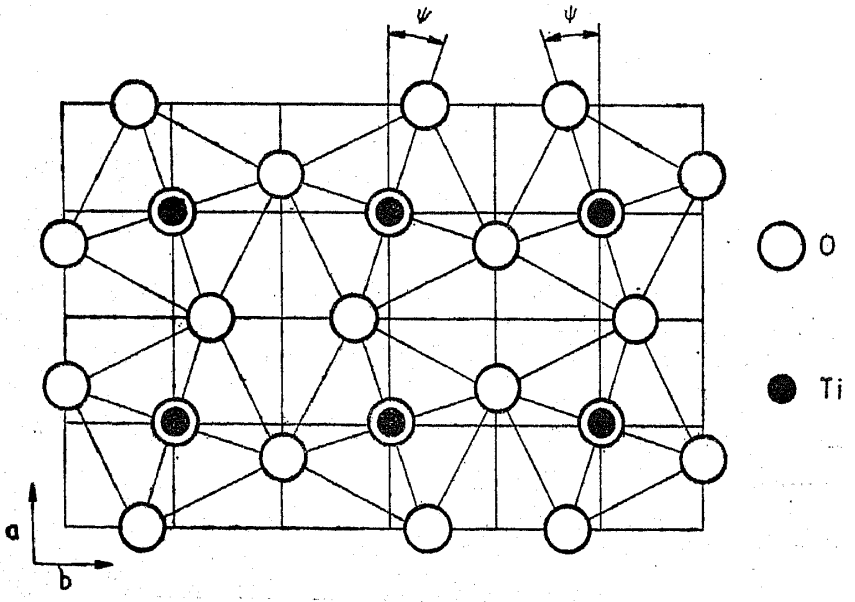

Figure 14. Schematic view of the rotated tetrahedra bel T_c in $SrTiO_3$

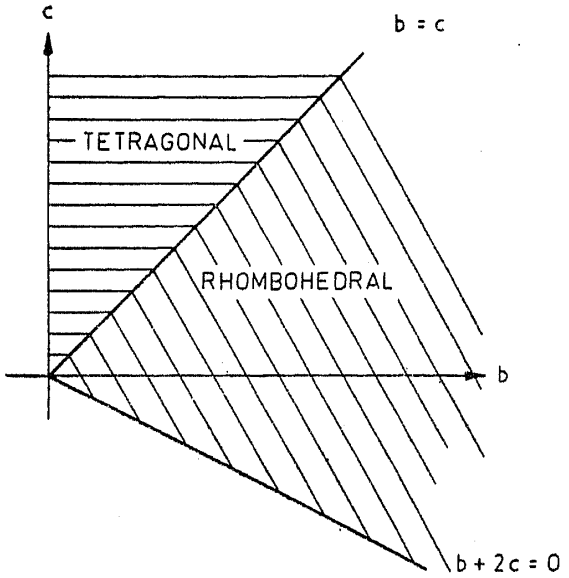

Figure 15. Stable regions of the tetragonal and rhombohedral phases of perovskite-type crystals, with respect to parameters occurring in the free energy expansion (eq. (25)).

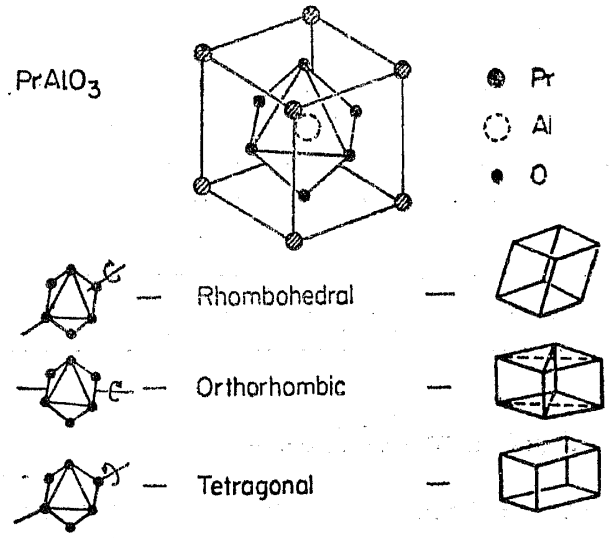

Figure 16. Cubic perovskite structure and the various other structures derivable from it by the rotation of the octahedra (After Birgeneau *et al* 1974).

Table 2. Phases of $CsPbCl_3$ (after Fujii *et al* 1974).

Phase I	$T > 47°$ C	Cubic	
Phase II	$47 > T > 42°$ C	Tetragonal	I → II first order Driven by M_3
Phase III	$42 > T > 37°$ C	Orthorhombic	II → III second order Driven by Z_5^x
Phase IV	$37°$ C $> T$	Monoclinic	III → IV first order Driven by Z_5^y.

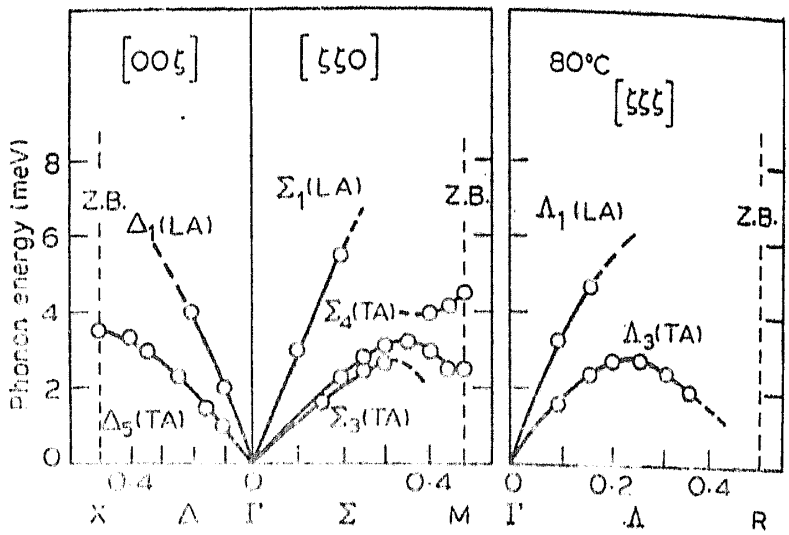

Figure 17. Dispersion relations for $CsPbCl_3$ at 80° C. The phonon which goes soft is of symmetry M_3 and is at the end of the Σ_3 (*TA*) branch (After Fujii *et al* 1974).

(-recall the case of $SrTiO_3$). The third transition at 37° C is triggered by the remaining member Z_5^y of the degenerate pair mentioned above. We thus find that condensation of rotational motions (of the oxygen tetrahedra) play a crucial role in these phase transitions. A better insight into the problem can be obtained by referring to figure 18 which shows the motions associated with the M_3 and R_{25} modes. Both involve rotations of the oxygen tetrahedra though with different phases. The structure that results from the successive rotations is shown in figure 19. Since M_3 and R_{25} both go soft, the order parameter in the free energy expansion must include contributions from both of these. Thus we write [equation (11)]

$$\delta\rho = \sum_i \psi\, \gamma_i \phi_i (M_3) + \sum_j \eta \delta_j \phi_j (R_{25}). \tag{26}$$

M_3 being nondegenerate, i runs only over all the wave-vectors belonging to the star of M. In the case of R_{25}, the degeneracy is three-fold and accordingly j should run over the manifold for every vector in the star of R. However, the star of R contains only one vector (R being on the zone boundary), and accordingly j runs only over the three components associated with the three-fold degeneracy of R_{25}. If (26) is used, the free energy expansion will involve powers of ψ and η, and suitable scalar invariant combinations of the γ_i's and δ_j's. From such an analysis, Fujii *et al* (1974) are able to obtain an adequate qualitative explanation of the various transitions observed by them.

7.4. *$BaTiO_3$*

It is unthinkable to discuss structural transitions in perovskite-type crystals without a reference to $BaTiO_3$, the most famous of them all ! Figure 20 shows a part of the phonon dispersion relations for $BaTiO_3$ from which it is clear that the softening occurs at the zone centre (Shirane *et al* 1967). The phonons in this case are overdamped.

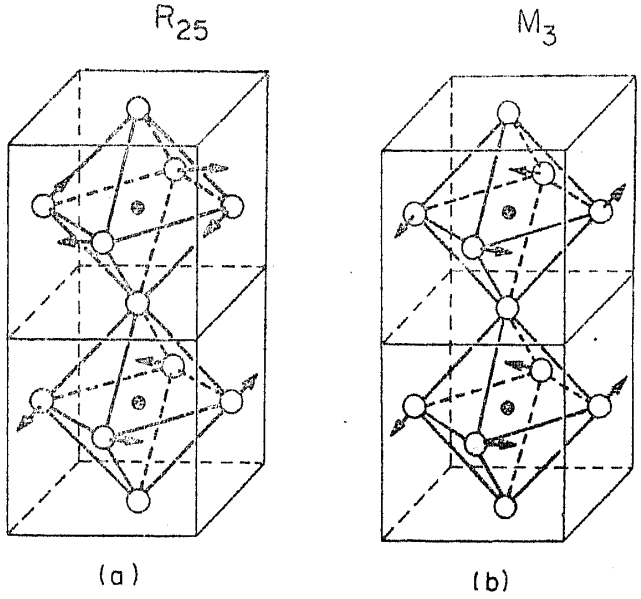

Figure 18. Displacement patterns of the X ion of ABX_3 for the R_{25} and M_3 modes (After Fujii *et al* 1974).

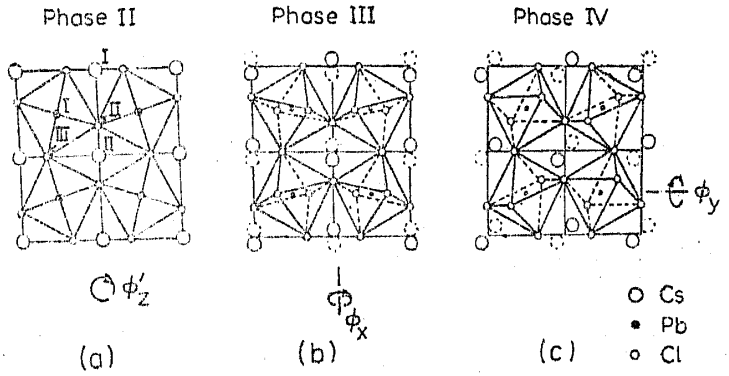

Figure 19. Arrangement of the $PbCl_6$ octahedra in the various phases of $CsPbCl_3$. All the three phase transitions involve the rotations of the octahedra. The concerned soft phonons are identified in table 2 (After Fujii *et al* 1974).

The phase transitions in $BaTiO_3$ show interesting correspondence to those of $CsPbCl_3$. In both, the transitions are due to the condensation of a triply degenerate mode. However in barium titanate the mode corresponds to the zone centre and transforms like a *polar* vector (-contrast with R_{25} where it transforms essentially like an axial vector) making ferroelectricity possible.

7.5. *$PrAlO_3$*

The last perovskite which I shall consider will be $PrAlO_3$ where electronic effects play an important role. $PrAlO_3$ is in fact claimed to be a classic example of co-operative John–Teller effect (CJTE) and since this subject will be covered by another speaker, I shall confine myself to pointing out the soft mode aspects.

$PrAlO_3$ exhibits several transitions—at 1320, 205 and 151 K. The 1320 K transition is due to the condensation of the R_{25} phonon, and results as in $LaAlO_3$,

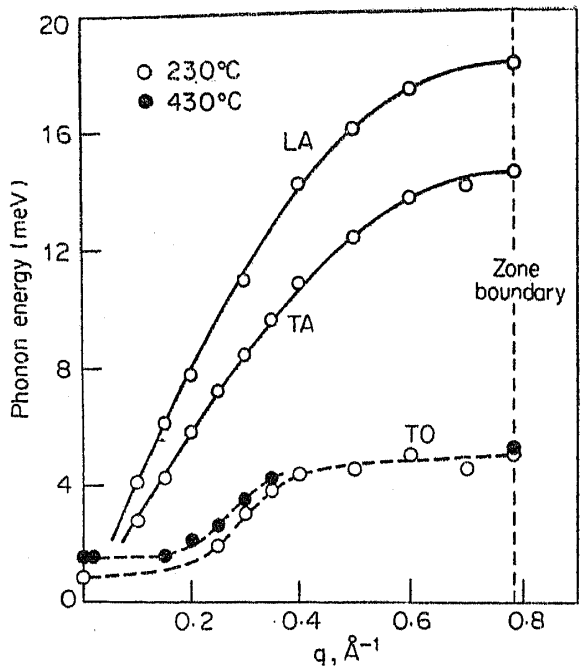

Figure 20. Soft modes in $BaTiO_3$ (After Shirane *et al* 1967).

in a cubic to rhombohedral change. In $LaAlO_3$, the rhombohedral structure survives till 0°K but in $PrAlO_3$ it does not. Based on fluoroscence, Raman scattering and other data, Harley *et al* (1973) concluded that the other transitions in $PrAlO_3$ arose explicitly on account of the coupling of the Pr^{3+} crystal field split levels to the R_{25} phonon. This last point needs some elaboration.

The Pr^{3+} ion has the $4f^2$ configuration, and the lowest free ion state $^3H_4$ is split corresponding to various crystal symmetries as shown in figure 21. Electronic transitions between the levels of an individual ion are possible (subject to selection rules), and in the crystal, these transitions can propagate leading to excitons. Figure 22 shows the dispersion curves for some of these excitons at 77° K. The coupling of the levels of one ion with those of another arises through the lattice, meaning that the excitons are hybrids of electronic transitions and phonons.

The lowest exciton in the rhombohedral phase is of particular interest. This results from a coupling of the $A_1 \rightarrow B_1$ transition (figure 21) with an optical phonon of B_1 symmetry. (R_{25} of the cubic phase splits into A_1, B_1 and A_2 in the rhombohedral phase). If the assertion of Harley *et al* (1973) is correct, then as the temperature is decreased to 151 K, this exciton branch should go soft. Neutron scattering experiments by Birgeneau *et al* (1974) reveal something slightly different. They find that it is not the exciton branch but rather an acoustic branch of the same symmetry which goes soft (figure 23), eventually causing the transition. The distortion resulting from the transition no doubt costs strain energy but the crystal gains in terms of electronic energy (figure 21). The usual JT distortion is local in character whereas here there is a cooperative effect involving the electrons in all the rare-earth ions on the one hand and the phonons on the other.

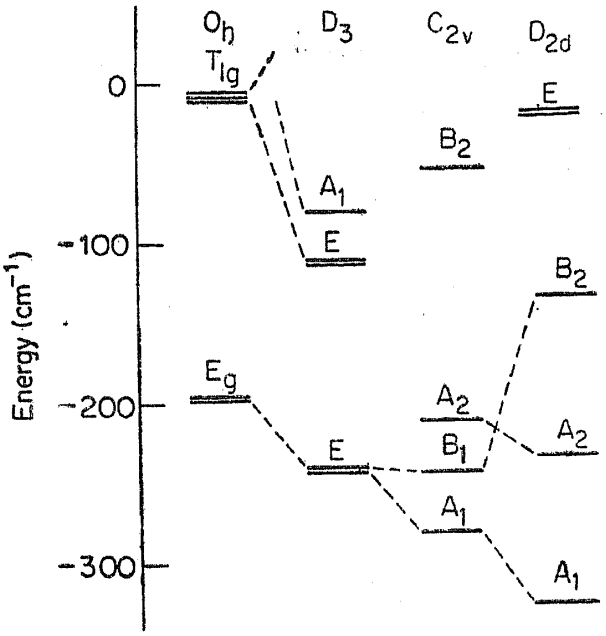

Figure 21. Low lying crystal field levels of $^3H_4$ multiplet of Pr^{3+} in the various principal symmetries of $PrAlO_3$. O_h corresponds to the cubic phase, D_3 to the rhombohedral, C_{2v} to the orthorhombic and D_{2d} to the tetragonal (After Birgeneau *et al* 1974).

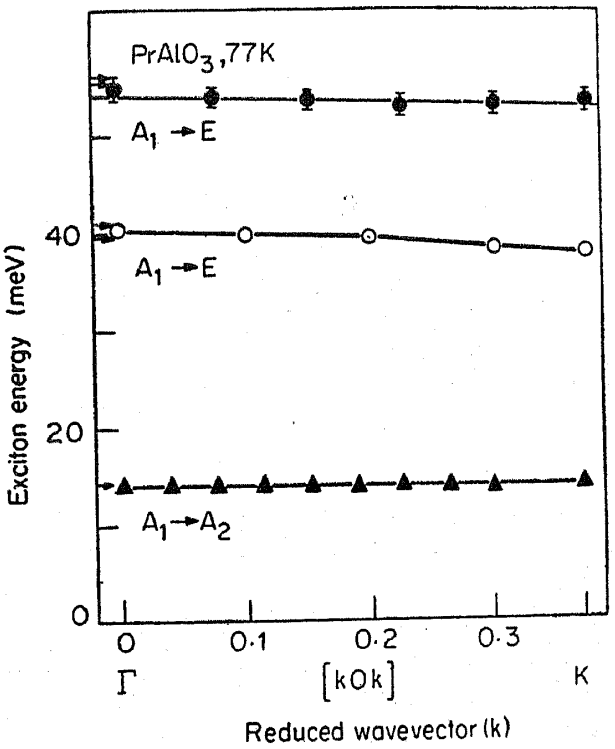

Figure 22. Dispersion relations along [kok] for some of the low frequency excitons in $PrAlO_3$ at 77 K. See also figure 21 (After Birgeneau *et al* 1974).

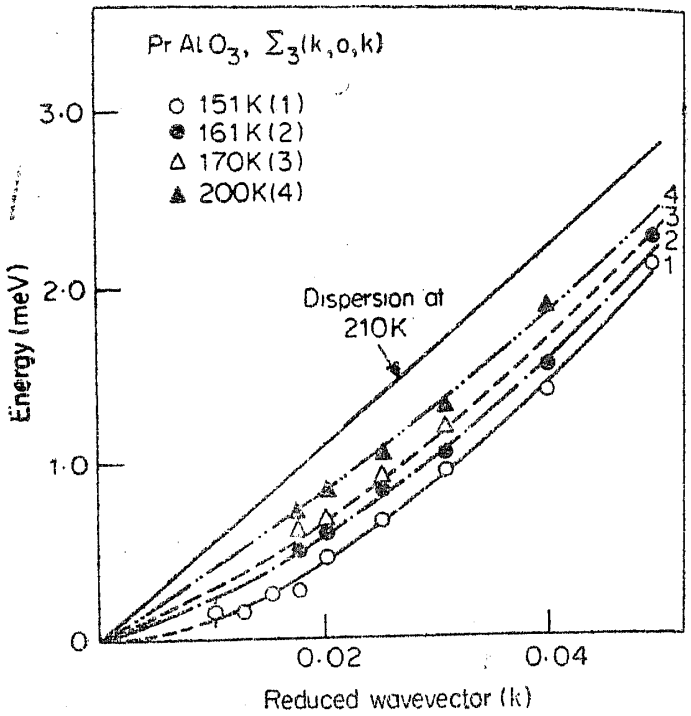

Figure 23. [101] acoustic phonon of $PrAlO_3$ which couples to the $A_1 \rightarrow B_1$ exciton. Observe the softening of the acoustic branch similar to what happens in Nb_3Sn (After Birgeneau *et al* 1974).

7·6. $Tb_2(MoO_4)_3$

I shall now move away from perovskites and look at another substance, namely $Tb_2(MoO_4)_3$ which also has unusual properties. At 159° C it undergoes a tetragonal to orthorhombic transition. In the low temperature phase, the substance is ferroelectric, and coupled with the two possible polarisation states $\pm P_z$, are the two mechanical configurations (figure 24) described by opposite shears ($\pm u_{xy}$). Just as the polarisation can be switched by an applied field, one mechanical configuration can be switched into another by an applied stress (ferro-elasticity). Further, both ferroelectricity and ferroelasticity are so coupled that P_z and u_{xy} change simultaneously.

Neutron scattering experiments by Dorner *et al* (1972) revealed that the phonon triggering the transition was at the zone boundary as may be seen from figure 25. Now a soft mode at the zone boundary usually results in an antiferroelectric structure [e.g. as in $(ND_4)D_2PO_4$] and cannot *directly* produce a spontaneous polarisation. However, the order parameter associated with the soft mode can couple with shear strain which in turn can produce polarisation by piezoelectric coupling. The free energy expansion must thus not only involve the order parameter ψ but also u_{xy} and P_z. The names secondary and tertiary order parameters have been suggested for the latter two. Other than those associated with the order parameter ψ, one has the additional equilibrium conditions

$$\partial g/\partial u_{xy} = 0; \quad \partial g/\partial P_z = 0.$$

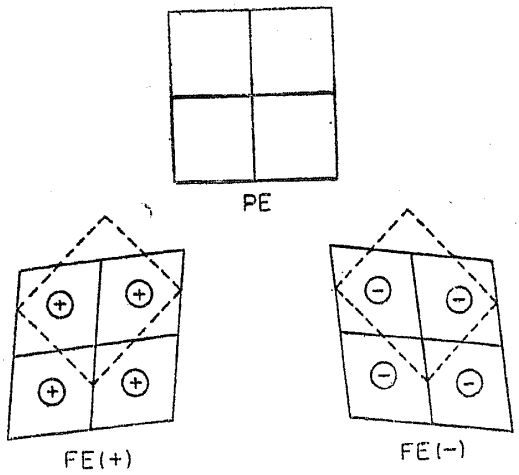

Figure 24. Sketch of the configuration of terbium molybdate in the para and ferroelectric phases. The solid lines in the lower half describe the unit cells of the paraphase and the dashed lines that of the ferrophase, projected on to the x–y plane. Observe the opposite shear of the two FE configurations (After Dorner *et al* 1972).

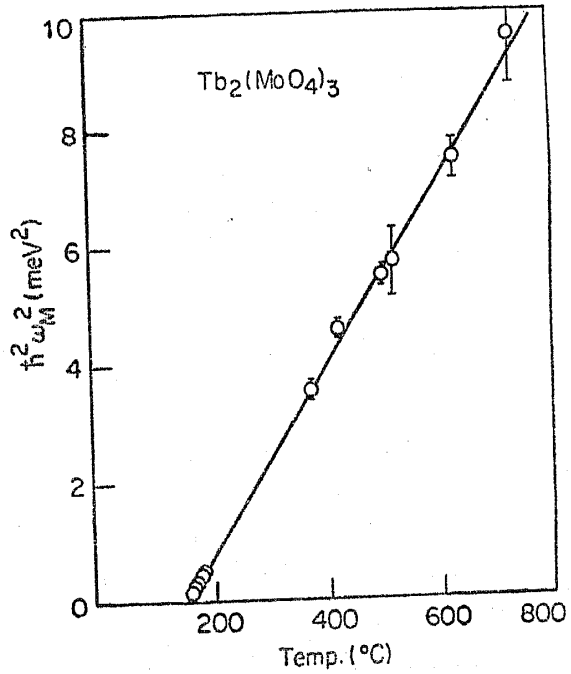

Figure 25. Temperature dependence of the soft mode at the point M in terbium molybdate (After Dorner *et al* 1972).

By using these, the free energy expansion can be expressed in terms of ψ alone, with suitably redefined expansion coefficients. Dorner *et al* (1972) have it in the form

$$g = \tfrac{1}{2}\ \omega_M^2\,\psi^2 + \tfrac{1}{4}\psi^4 \sum_\alpha B_\alpha f_\alpha^4(\gamma_i)$$

$$+ 1/6\,\psi^6 \sum_\alpha W_\alpha f_\alpha^6(\gamma_i) + \cdots$$

where ω_M, B_α and W_α are suitably defined coefficients. Having eliminated the secondary and tertiary order parameters, the analysis can be carried out as usual. Among other things, knowing the values of the coefficients, the soft mode frequencies in the two phases can be calculated [recall equation (15)]. Figure 26 shows a schematic plot of what can result.

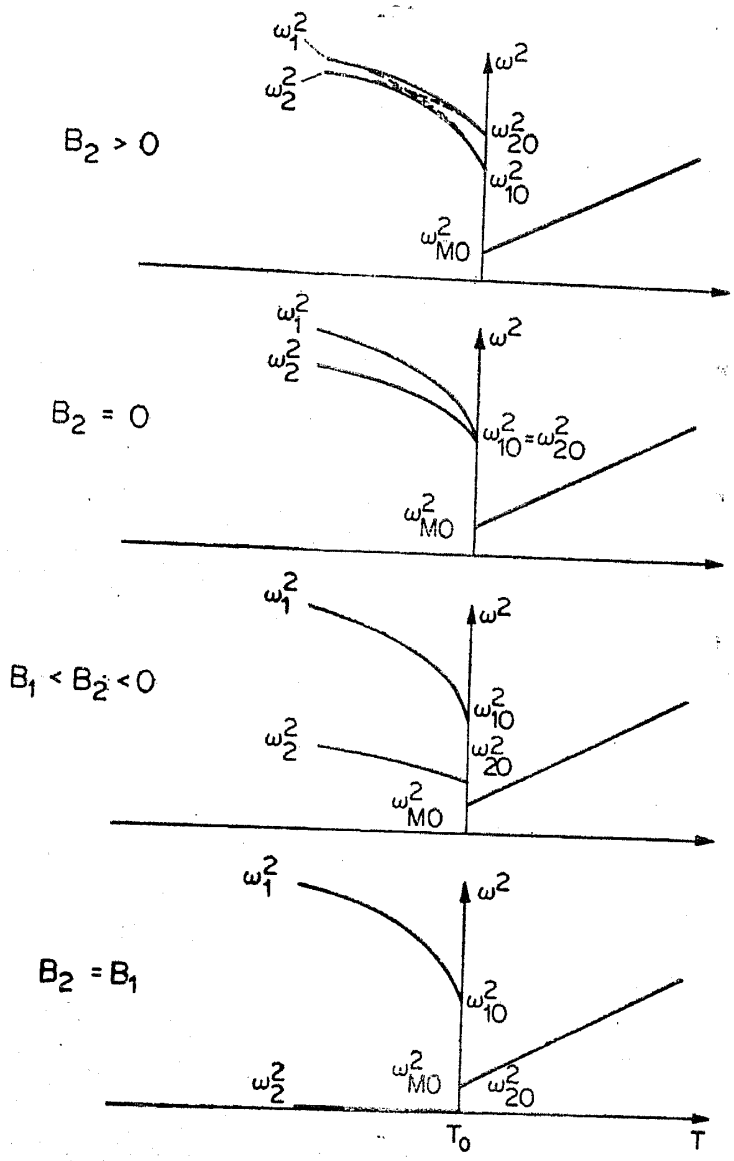

Figure 26. Soft-mode frequencies in the para- and ferro-phases of terbium molybdate. Depending on the parameter values, various situations can arise (After Dorner *et al* 1972).

One of the distinguishing features of this experiment is the close correspondence established by Dorner *et al* (1972) between the displacements of the atoms in the soft mode vibrations of the high temperature phase, and the *static* displacements of the atoms in the ferroelectric phase with respect to positions occupied in the paraelectric phase. The displacement amplitudes associated with the soft mode were determined by resorting to what may be called generalised crystallography

(Brockhouse 1961). In this, one measures the soft phonon intensity at several equivalent points in reciprocal space similar to the manner in which crystallographers measure the intensity of different Bragg reflections. From a study of such intensities, the eigenvector of the phonon may be determined and hence the vibration amplitudes. Dorner *et al* (1972) note that the amplitudes so determined are close to displacements deduced from a comparison of the (static) structures in the two phases. There was however no complete agreement; among other things, this could be due to the soft mode coupling slightly with other phonons to produce the transition.

7·7. K_2SeO_4

The last example I shall consider in the present series will be that of K_2SeO_4. This substance undergoes two successive phase transitions at 129·5 K and 93 K, the latter being a ferroelectric phase transition, with spontaneous polarisation along the *c* axis. In the phase above 129·5 K, the crystal has the orthorhombic structure, and as the temperature is lowered, a soft mode appears. Interestingly, this is neither at the zone centre or the zone boundary as in the examples discussed so far. The softening occurs at a somewhat odd value of q (figure 27), which has important consequences to the phase that develops below 129 K which is referred to as an incommensure phase by Iizumi *et al* (1977).

Let us look at this situation somewhat more closely. Figure 28 shows a portion of the reciprocal lattice of the orthorhombic phase. On the right hand side is shown the corresponding lattice for the ferroelectric phase. Referring back to figure 27, we find that the minimum of the soft Σ_2 branch changes with temperature though it is close to $q = (1/3, o, o)$. The displacement δ from this point (figure 28) decreases with temperature in the manner indicated in figure 29. In the incommensurate phase, a satellite Bragg reflection develops in this region of

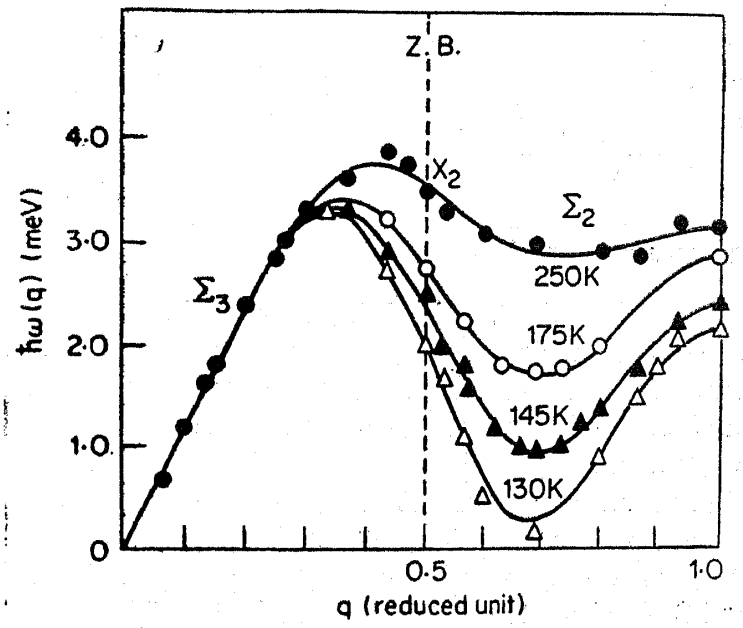

Figure 27. Dispersion relation of the Σ_2 soft mode in K_2SeO_4 (After Iizumi *et al* 1977).

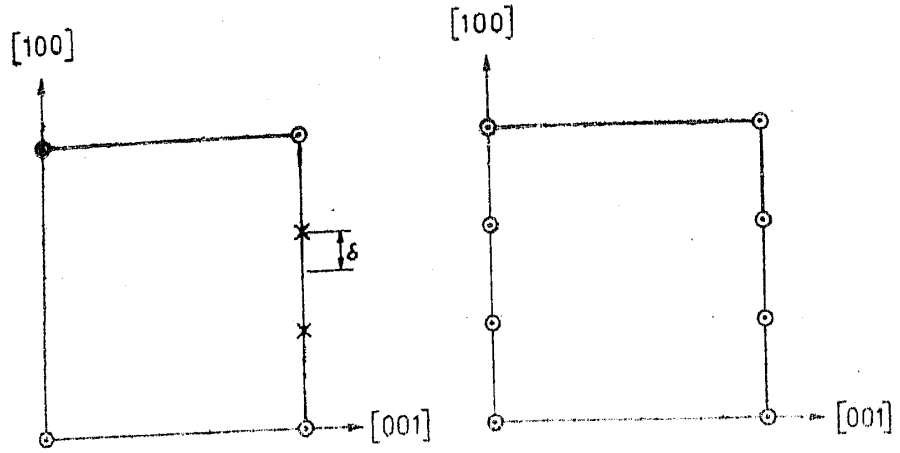

Figure 28. Portion of the (010) plane in the reciprocal lattice of K_2SeO_4. On the left is the lattice for the high temperature phase and on the right that for the ferroelectric phase. In the high-temperature phase, a softening occurs at a point displaced by δ from $q = (1/3, 0, 0)$, shown by cross. In the incommensurate phase, a satellite reflection developes at X. δ is a function of temperature.

reciprocal space and if this satellite reflection is followed as a function of temperature, it indicates a further decrease of δ as may be seen in figure 29. Finally, at 93 K, δ becomes zero discontinuously leading to a incommensurate to commensurate phase transition, and a concomitant ferroelectric behaviour. Iizumi *et al* (1977) also establish that an interaction term of the form $C(\psi^3(q) + \psi^3(-q))P_z$ in the free energy expansion is crucial to an explanation of the two transitions.

I hope I have given enough of a sampling of experiments to convey the fact that very interesting and very exciting developments have occurred during the past decade in the subject of structural phase transitions. I must at this point express my apologies for projecting mainly the results of neutron scattering experiments (which should be understandable in view of my earlier background). I assure you however that no slight is intended to the other techniques! I also freely admit that these techniques too have made important contributions and I shall make partial amends by referring to some of these in the context of the central peak, to which I now direct attention.

8. Concerning the central peak

At a conference on soft modes held in Geilo, Norway in 1971, Riste *et al* (1971) sprung a surprise by announcing that soft modes had a companion in the shape of a zero-frequency peak. This phenomenon, known as the central peak, has created considerable interest. Initially there was some speculation that the central peak could be due to defects, etc., but since then the existence of this phenomenon has been confirmed in a number of cases and the possibility of defects producing spurious effects has been ruled out. Also there are theoretical grounds for believing in the existence of the central peak in three as well as lower dimensional systems (Krumhansl and Schrieffer 1975; Schneider and Stoll 1976). There is as yet no complete understanding of the phenomenon which is why it is continuing to attract attention.

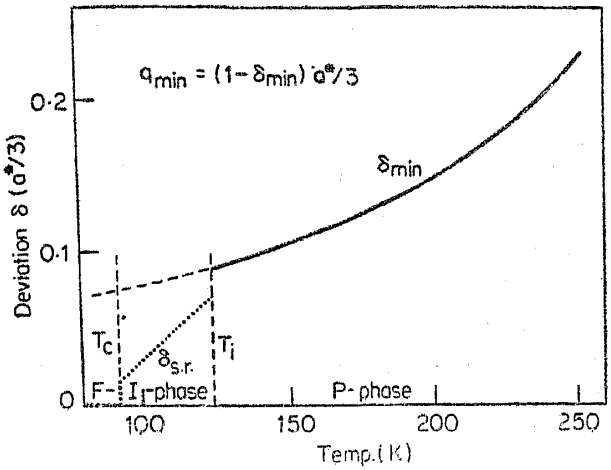

Figure 29. Variation of δ (see figure 28) with temperature. Above 130 K it is determined from the minimum of the soft branch. In the incommensurate phase it is determined from the position of the satellite reflection (After Iizumi *et al* 1977).

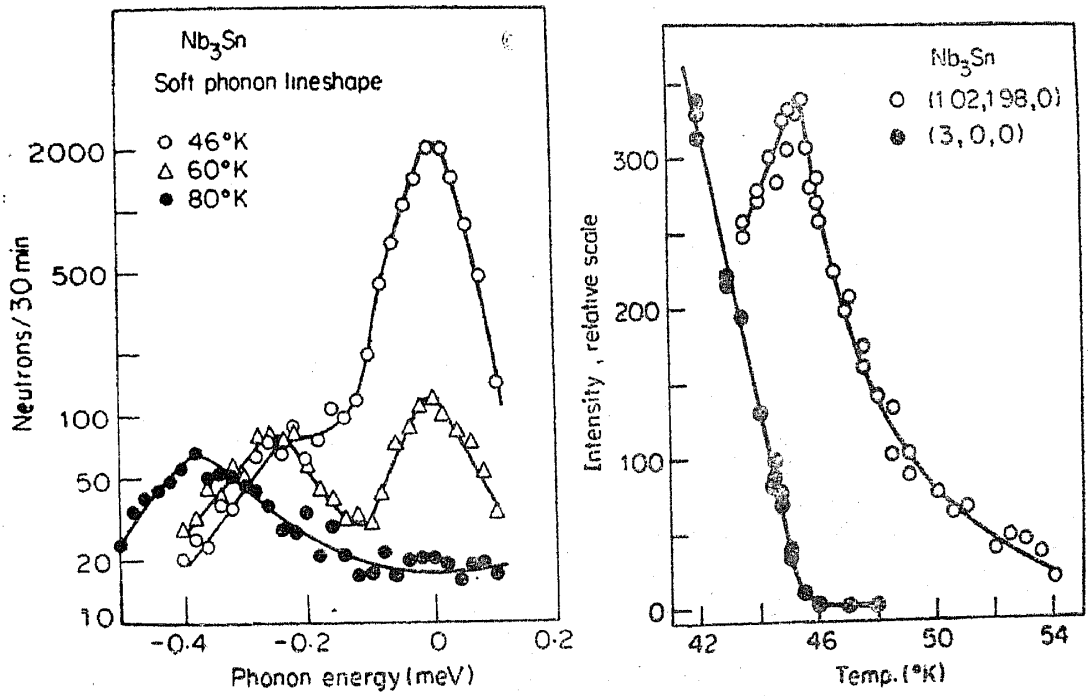

Figure 30. (*a*) Spectra of neutrons scattered by soft mode phonons in Nb_3Sn at several temperatures above T_m. Observe the development of the central peak. (*b*) The open circles represent the temperature dependence of the intensity of the central peak while the closed circles show the onset of the structural phase transition as monitored by the forbidden (300) reflection (After Axe *et al* 1974).

Let us first briefly review some of the experimental results concerning the central peak. Figure 30 *a* shows the neutron scattering spectrum for Nb_3Sn at several temperatures close to the martensitic transformation temperature T_m. It is quite clear that as $T \to T_m^+$, a central peak develops whose intensity rapidly grows as brought out in figure 30 b.

Figure 31 shows some results for $KMnF_3$ near the transition at 90°K (which is associated with a soft mode at the point M in the Brillouin zone). Here the soft mode is not very evident because it is overdamped. A careful examination of the broad base however reveals its existence. The point to note in the figure is that even in the case of overdamped soft modes, there is a central peak.

Figure 32 shows some results on light scattering from $SrTiO_3$. The critical opalescence which is reminiscent of scattering from liquids, arises in the present instance due to the central peak. Of interest is the fact that the central peak exists both below and above T_c.

To analyse the observations in a quantitative way, Shapiro *et al* (1972) write the one-phonon cross-section (for neutron scattering) as

$$S(q, \omega) = \frac{\hbar}{\pi}(1 + n(\omega))\, I_m [\Omega^2(q) - \omega^2 + \pi(q, \omega, T)]^{-1},$$

$$n(\omega) = [\exp(\hbar\omega/k_B T) - 1]^{-1}. \tag{27}$$

They further assume

$$\pi(q, \omega, T) = [\triangle(q, T) - i\omega\Gamma_0(T)] - \frac{\gamma\delta^2(T)}{\gamma - i\omega}. \tag{28}$$

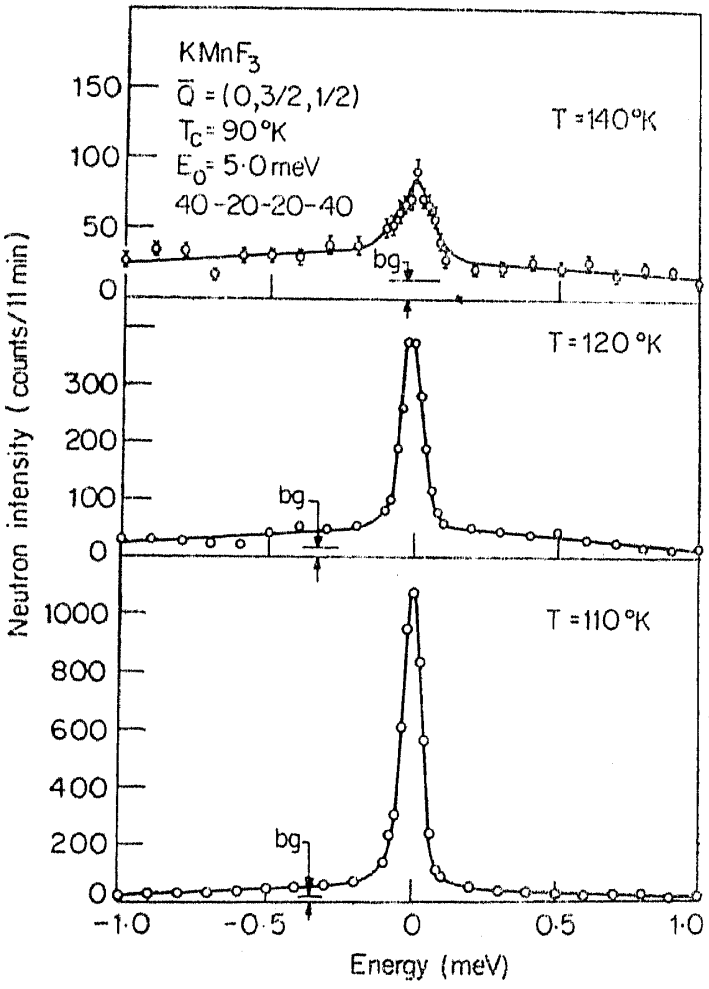

Figure 31. Scattered neutron spectra of $KMnF_3$ at $q = q_m$ at several temperatures above the transition temperature (After Shapiro *et al* 1974).

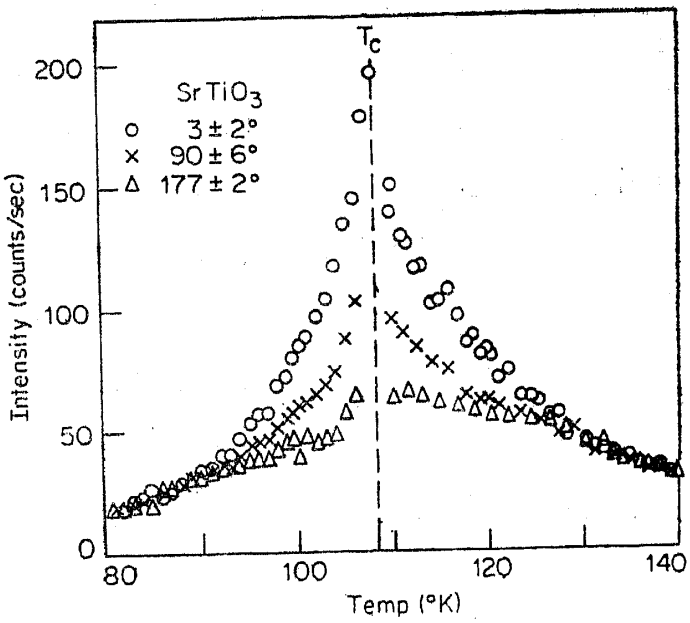

Figure 32. Intensity of light scattering from $SrTiO_3$ as a function of temperature for the three scattering angles (After Steigmeier *et al* 1974).

Here, the term Δ produces as usual a frequency shift given by

$$\omega_\infty^2 = \Omega^2 + \Delta, \tag{29}$$

while Γ_0 as usual contributes to damping. The third term on the r.h.s. is an additional contribution to damping due to coupling with (an unspecified) mode with a Debye-type relaxation spectrum.

Introducing $\omega_0^2 = \omega_\infty^2 - \delta^2$ and taking $(k_B T/\hbar\omega) \gg 1$, $\Gamma_0 \ll (\delta^2/\gamma)$ and $\omega_\infty^2 \gg \gamma$, $S(q, \omega)$ separates into two parts, S_{central} and $S_{\text{side band}}$. These are respectively given by:

$$S_{\text{central}} = \frac{k_B T}{\pi} \frac{\delta^2}{\omega_0^2 \omega_\infty^2} \frac{\gamma^1}{\omega^2 + \gamma^{12}}, \quad \gamma^1 = \frac{\omega_0^2}{\omega_\infty^2} \gamma, \tag{30}$$

$$S_{\text{side band}} = \frac{k_B T}{\pi} \frac{\Gamma_0}{(\omega_\infty^2 - \omega^2)^2 + \omega^2 \Gamma_0^2}. \tag{31}$$

The fractional integrated central peak intensity is

$$r(q) = \frac{I_{\text{central}}}{I_{\text{total}}} = \frac{\int S_{\text{central}}\, d\omega}{\int S_{\text{side band}}\, d\omega} = \frac{\delta^2}{\omega_\infty^2}. \tag{32}$$

Many features emerge from this analysis. First is that when $T \gg T_c$, $\omega_\infty^2 \gg \delta^2$ whence there is very little manifestation of the central peak. (Note, incidentally that $\omega_0 \approx \omega_\infty$ in this situation). However, as $T \to T_c^+$, $\omega_\infty \to \delta$ and consequently the central component grows.

The second point is that when $T \sim T_c$, different probes see the situation in the medium differently. Directing attention to Nb_3Sn as an example, a high-frequency probe like neutron scattering sees the mode frequency as ω_∞ and correspondingly

yields a value $v_\infty = (\omega_\infty/q)$ for the mode propagation velocity. On the other hand, an ultrasonics experiment sees the mode frequency as yielding a value $v_0 = (\omega_0/q)$ for the velocity. That these two velocities are different is clearly brought out in figure 33. From the definition of ω_0 and ω_∞ we know that

$$v_\infty^2 = v_0^2 + [\delta^2(q)/q^2].$$

By measuring the ratio $r(q)$ as a function of q, Axe *et al* (1974) were successfully able to determine (δ^2/q^2), and thereby reconcile the difference between the high and low frequency velocities.

One question which has often been raised is whether the central peak has a width. No doubt the above analysis suggests that the width is finite but one would like an experimental confirmation of this as well. On account of its limited energy resolution, neutron scattering has not been able to provide anything more than a suggestive answer. EPR techniques, on the other hand, have provided a clearer picture. As an illustration let us consider the case of $SrTiO_3$ doped with Fe^{3+} ions. The ions enter the Ti site substitutionally, and when there is a nearest neighbour oxygen vacancy, EPR becomes possible. The spectrum reflects the local orientation of the oxygen tetrahedra, and fluctuations in the orientation (*i.e.*, fluctuations in the order parameter) then produce a fluctuating magnetic field at the site leading to line broadening. If H_0 denotes the static magnetic field and H_r the resonance field, then (Blinc and Zeks 1974)

$$H_r(t) = H_0 + A\psi(l, t) \tag{33}$$

where A is an appropriate constant and l denotes the lattice site. The second moment $\langle(\delta H)^2\rangle$ of the line is given by

$$\langle(\delta H)^2\rangle = \langle(H_r - H_0)^2\rangle = A^2\langle\psi(l, t)\psi(l, t)\rangle. \tag{34}$$

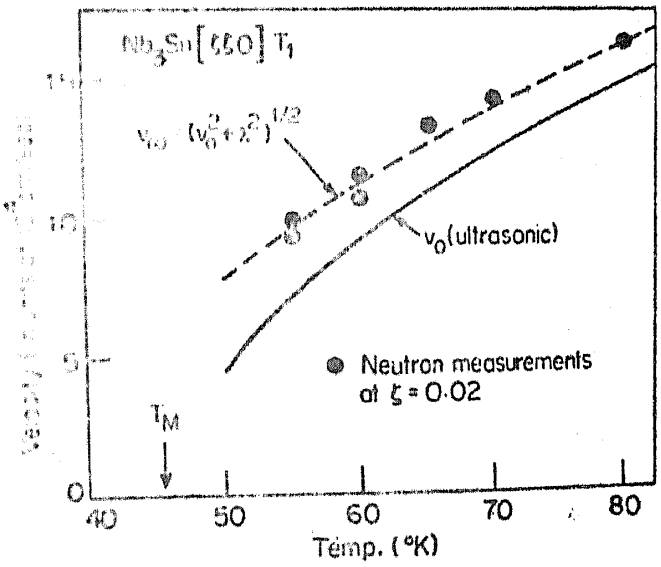

Figure 33. Velocity of [110] acoustic phonons in Nb_3Sn. The velocity difference between the neutron and ultrasonic results can be explained by taking into account the central peak. (After Axe *et al* 1974).

Defining

$$S_{\psi\psi}(\mathbf{q}, \omega) = \int \exp[i(\mathbf{q}\cdot\mathbf{r} - \omega t)] \langle \psi(\mathbf{r}, t)\psi(0, 0)\rangle \, d\mathbf{r}dt, \tag{35}$$

and

$$J(\omega) = \sum_{\mathbf{q}} S_{\psi\psi}(\mathbf{q}, \omega)^*, \tag{36}$$

we obtain,

$$\begin{aligned}\int_{-\infty}^{\infty} J(\omega)\, d\omega &= 2\int_{0}^{\infty} J(\omega)\, d\omega, \\ &= \langle \psi(l, t)\psi(l, t)\rangle, \\ &\approx 2\int_{0}^{\omega_M} J(\omega)\, d\omega.\end{aligned}$$

Combining (35) and (36) we see that the line width is determined by the extent to which the measuring system (characterised by a frequency ω_M) sees the central peak.

Figure 34 shows $J(\omega)$ for two temperatures. When $T \ll T_c$, we observe that there are many components in the (q-integrated) central peak with frequencies higher than ω_M which therefore do not contribute to the line width. This is the so-called fast-motion region where one obtains a relatively narrow line. On the other hand when $T \sim T_c$, the situation changes to that in figure 34 b, and the entire central peak now contributes to the line width. The observed line width as a function of

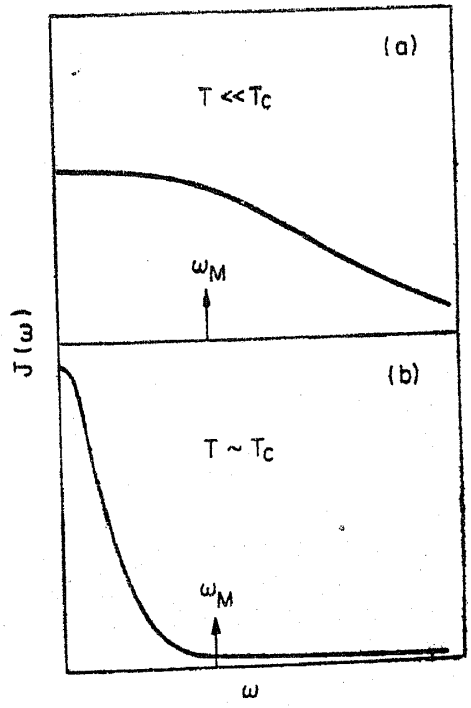

Figure 34. Sketch of $J(\omega)$ for (*a*) $T \ll T_c$ and (*b*) $T \sim T_c$. ω_M is the measuring frequency.

* In practice, the sum over q will range only over a small region of q-space since the central peak occurs only when $q \approx q$ (soft mode).

temperature is shown in figure 35 where the existence of the slow- and fast-motion regions is clearly brought out. From such an analysis, it has been estimated that for $T = T_c + 0{\cdot}8°$ K, for example, the central peak has a width of 70 MHz which is too small to be seen by neutron scattering.

Turning now to the theories concerning the central peak, the basic idea underlying all these is existence of two time-scales in the relaxation of the order parameter or the soft mode (as the case may be).* The appearance of two time-scales is visualised as due to coupling with a slowly relaxing variable A. The latter is usually chosen to be a conserved quantity since we know from hydrodynamics (see, for example Forster 1975) that the relaxation time for the $q \to 0$ fluctuations of such a quantity is very long. This coupling between the slow variable and the primary quantity then results in a peak at $\omega = 0$, which becomes stronger as the frequency of the soft mode itself starts approaching zero (since the interaction then becomes easier).

Now for the soft mode to couple with another (slowly changing) variable, one important requirement is that such a coupling must be permitted by symmetry i.e. the two entities must transform according to the *same* irreducible representation of the symmetry group of the phase under consideration. This restriction is important because at first sight one might be tempted to imitate what is done for liquids where the central peak (usually called the Rayleigh peak) is well-known and arises due to coupling with temperature fluctuations. On the other hand, symmetry might forbid such a direct coupling to temperature fluctuations. Further comments on this will be made later.

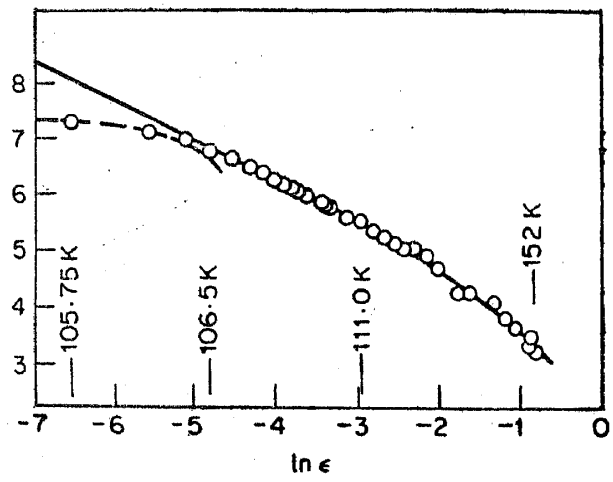

Figure 35. EPR linewidth in $SrTiO_3$ as a function of temperature (expressed in terms of $\epsilon = (T_c - T)/T$). The dots are experimental points. Theoretical curves for fast (solid line) and slow (dotted line) motions are also shown (After Muller 1974).

* The analysis of the central peak may be done either in terms of the dynamics of the soft mode normal coordinates or that of the order parameter itself. As already noted [(11) and (12)] the two are closely linked. Experiments like neutron scattering directly probe the vibrations, and for this reason theories of central peak are usually formulated using the normal coordinates of the soft mode as the dynamical variable.

First let us try to understand the physics underlying the origin of the central peak by considering an analogous example from magnetism, namely the case of MnF_2 (Heller 1970). As we are all aware, this substance becomes antiferromagnetic below $\sim 67{\cdot}5°$ K. Figure 36 shows its longitudinal and transverse susceptibility; we shall focus attention on the longitudinal part. We imagine now that a staggered magnetic field (i.e. a spatially varying one) nearly synchronous with the spin alternation is applied parallel to the antiferromagnetic axis, and then switched off after equilibrium is established. The system will now relax towards a new equilibrium. Heller has argued that the relaxation of the longitudinal component of the magnetisation will have the behaviour shown in figure 37 a, i.e. exhibit two time scales. What happens is that as soon as the applied field is removed, the different parts

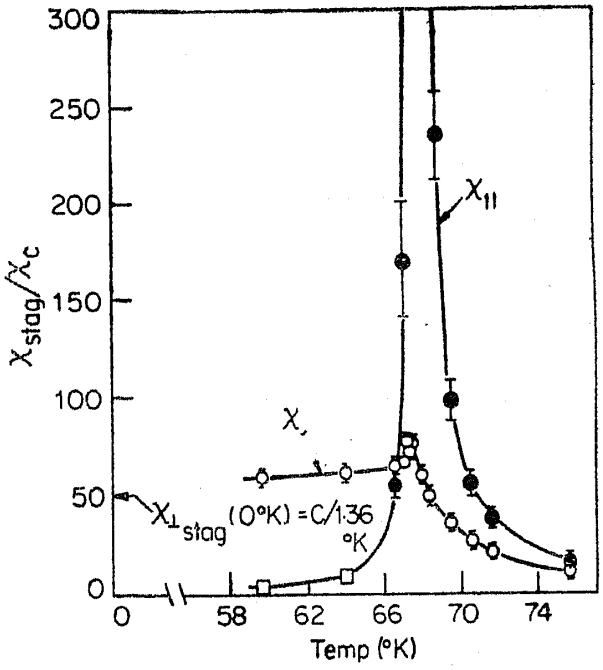

Figure 36. Transverse and longitudinal staggered susceptibilities in MnF_2 (After Heller 1970).

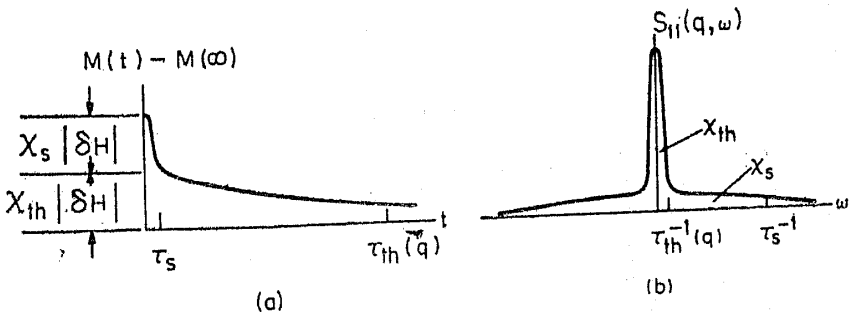

Figure 37. Relaxation of the local staggered magnetisation following the turning off of the exciting field. Observe the presence of two time scales. This leads to a longitudinal scattering function with a narrow central peak as sketched in (*b*) (After Heller 1970).

of the system relax rapidly in an adiabatic fashion. Because of the fact different parts of the system were initially exposed to different fields (owing to its oscillatory nature), there would exist after the completion of the first phase, variations in temperature between different parts of the crystal. These temperature fluctuations then start evening out in a gradual manner producing the second component in the relaxation. The net result is that the power spectrum will have two distinct components as sketched in figure 37 b. Essentially a similar thing happens in the case of the soft mode also; only that here we have to consider the relaxation of an oscillator. Normally, such an oscillator when excited and let go will exhibit an oscillatory decay, and its power spectrum would show a peak at the oscillator frequency, with a width related to the decay constant. When coupled to a slowly relaxing variable, the decay characteristic may be expected to be altered as sketched in figure 38 a, leading to a spectrum as in figure 38 b.

An analysis due to Feder (1974) provides substance to the above qualitative remarks. Feder considers a model Hamiltonian (potential energy terms only) of the form

$$\frac{1}{2}\sum_{l}\left(\Omega_0^2 Q_l^2 + \tfrac{1}{2}\gamma Q_l^4\right) - \frac{1}{2}\sum_{ll'} Q_{l'} J_{ll'} Q_l \quad , \tag{37}$$

where Q_l is a local normal coordinate at lattice site l. For example, one could think of it as being proportional to the rotation angle of the oxygen octahedra in

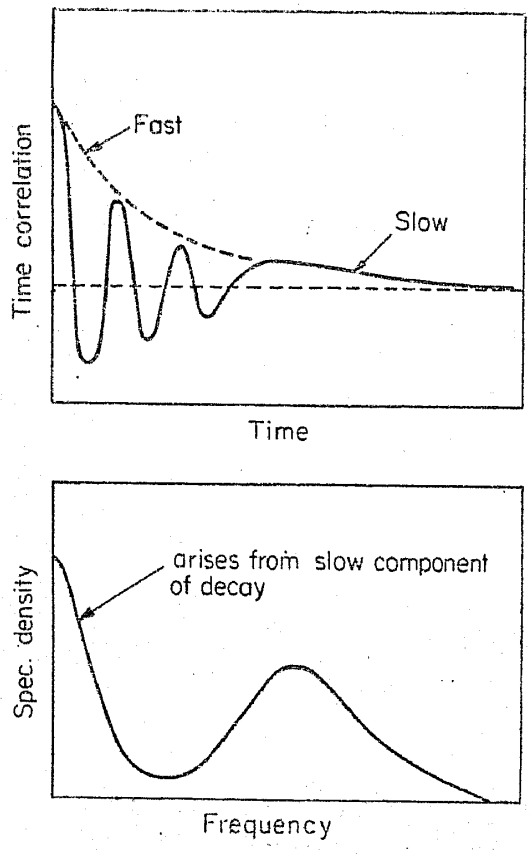

Figure 38. Schematic drawing of the time decay of the order parameter correlations, and its power spectrum.